Deep-Sea Research II 58 (2011) 999–1018

Contents lists available at ScienceDirect

Deep-Sea Research II

journal homepage: www.elsevier.com/locate/dsr2

The influence of winds, sea-surface temperature and precipitation anomalies on Antarctic regional sea-ice conditions during IPY 2007

Sharon Stammerjohn [a,*], Ted Maksym [b], Petra Heil [c], Robert A. Massom [c], Martin Vancoppenolle [d,e], Katherine C. Leonard [f,g]

[a] Ocean Sciences Department, University of California Santa Cruz, Santa Cruz, CA, USA
[b] British Antarctic Survey, High Cross, Madingley Road, Cambridge, UK
[c] Antarctic Climate and Ecosystems CRC & Australian Antarctic Division, c/o University of Tasmania, Sandy Bay, Tasmania, Australia
[d] Institut d'Astronomie et de Géophysique G. Lemaître, Université Catholique de Louvain, Louvain-la-Neuve, Belgium
[e] Department of Atmospheric Sciences, University of Washington, Seattle, WA, USA
[f] Lamont-Doherty Earth Observatory of Columbia University, Palisades, NY, USA
[g] WSL Institute for Snow and Avalanche Research SLF, Davos, Switzerland

ARTICLE INFO

Article history:
Received 9 October 2010
Accepted 9 October 2010
Available online 21 October 2010

Keywords:
Antarctic sea ice
Antarctic ice drift
Snow on sea ice
Ocean-ice-atmosphere system

ABSTRACT

The 2007 International Polar Year (IPY) in the Antarctic was distinguished by strong regional and seasonal ice-atmosphere-ocean anomalies associated with an overall weakening of the prevailing westerly circulation. Here we assess the ice-atmosphere-ocean conditions leading up to and during two IPY field campaigns that took place in early spring (September-October): the U.S.-led Sea Ice Mass Balance Antarctica (SIMBA, 68-72°S, 90-95°W) and the Australian-led Sea Ice Physics and Ecosystems eXperiment (SIPEX, 63-67°S, 115-130°E). Our regional analysis is presented within the context of circumpolar and inter-annual variability relevant to other IPY Antarctic studies. Using satellite-derived and numerically analyzed surface and atmospheric variables, we examine relationships between (i) winds and sea-ice concentration and drift, (ii) sea-surface temperature and ice-edge anomalies, and (iii) precipitation and snow accumulation. Though Antarctic-averaged sea-ice extent in September 2007 was the second highest observed for 1979-2007, the SIMBA and SIPEX studies sampled the two regions showing the largest negative sea-ice anomalies in the Southern Ocean. Maps of sea-surface temperature (SST) and sea-ice concentration (SIC) anomalies revealed distinct regional patterns, showing warm SST/low SIC in the greater SIMBA (including all of the Bellingshausen and Amundsen seas) and western SIPEX regions, versus cool SST/high SIC in the Weddell, Ross and eastern SIPEX regions. In the SIMBA and western SIPEX regions, warm northerly winds in May (overlying the warm SSTs) brought anomalously high precipitation to those regions, but due to the regional delays in sea-ice advance (by up to 2 months), most fell on open ocean, which in turn contributed to negative and near-zero September snow depth anomalies in those two regions, respectively. During autumn (March to May), warm SSTs offshore of those regions extended from mid-to-high latitudes, resulting from meridional advection of heat associated with a wave-3 atmospheric circulation pattern. In the SIMBA and SIPEX regions, the late sea-ice advance followed unusually long ice-free summer periods, which suggests that solar ocean warming was relatively high in those regions. The warm ocean conditions may help to explain why the ice edge remained well south of its mean position despite instances during winter of cold southerly winds and northward sea-ice drift. Finally, with respect to the 1978-2008 record, year 2007 was a continuation of decreasing sea ice in the SIMBA region (e.g., decreased annual sea-ice extent and ice season duration), whereas in the SIPEX region, year 2007 was a negative departure from an otherwise slightly positive trend in annual sea-ice extent and ice season duration.

1. Introduction

With the ability to continuously monitor sea-ice conditions from space starting in the early 1970s, it has been known that Antarctic sea ice exhibits high regional and seasonal variability resulting from a complex interplay between atmospheric and oceanic forcing (e.g., Zwally et al., 1983). Here, we focus specifically on how winds, sea-ice drift, sea-surface temperature, and precipitation shaped regional sea-ice conditions leading up to and during two International Polar Year (IPY) field campaigns that took place in early spring (September-October 2007) in seasonal sea-ice zones on opposite sides of the Antarctic continent. The U.S.-led Sea

* Corresponding author. Tel.: +1 845 365 8353; fax: +1 845 365 8736.
E-mail address: sharons@ldeo.columbia.edu (S. Stammerjohn).

0967-0645/$ - see front matter © 2010 Elsevier Ltd. All rights reserved.
doi:10.1016/j.dsr2.2010.10.026

Ice Mass Balance Antarctica (SIMBA, 68-72°S, 90-95°W) field study was a time series drift experiment that took place within pack ice of the Bellingshausen Sea from 24 September to 27 October 2007 (Fig. 1A) (Lewis et al., 2011). The direction of SIMBA's month-long drift track was predominantly wind-driven and westward along the Bellingshausen continental shelf slope, with one northeast then southwest drift excursion. The Australian-led Sea Ice Physics and Ecosystems eXperiment (SIPEX, 63-67°S, 115-130°E) conducted 15 separate ice stations within the relatively narrow (north-south) seasonal sea-ice zone off East Antarctica from 9 September to 11 October 2007 (Fig. 1B) (Worby et al., in press). Apart from one fast-ice station, all stations were within the pack ice and mostly along the continental shelf slope. Though sampling strategies were different between the two projects, scientific objectives were similar and focused on understanding the physical and biogeochemical processes within the sea-ice environment, the couplings between them, and how these may be altered by climate change.

Here we present a regional and circumpolar assessment of sea-ice conditions during IPY 2007 that complements detailed *in situ* snow and sea-ice studies (e.g., Leonard and Cullather, 2008; Lewis et al., 2011; Toyota et al., in press; Worby et al., in press; Xie et al., 2011, and others in this volume) and provides the contextual environmental setting for the physical, biological and biogeochemical parameters and processes observed and measured during SIMBA, SIPEX and other Antarctic field campaigns in 2007. Our examination of how winds, sea-ice drift, sea-surface temperature, and precipitation affected regional sea-ice conditions within the context of circumpolar variability and known climate anomalies during IPY 2007 (e.g., Levinson and Lawrimore, 2008) is also relevant to the study of sea-ice processes in general. Whereas wind forcing is typically the dominate control determining sea-ice extent and length of ice season (e.g., Massom et al., 2008; Stammerjohn et al., 2008), precipitation, and hence, snow depth, exert considerable control on the growth and development of Antarctic sea ice (Sturm and Massom, 2009). The insulating effect of snow limits ice growth (e.g., Fichefet et al., 2000), but can also contribute significantly to thickening through snow ice formation (Maksym and Jeffries, 2000). Snow-ice formation also plays an important role in governing sea-ice ecosystems (e.g., Fritsen et al., 1994). There also is some suggestion that increased snowfall will lead to greater sea-ice extent (e.g., Fichefet and Morales Maqueda, 1999). Therefore, within this context, we include an analysis of precipitation and snow depth, alongside winds and sea-surface temperature, in our discussion of factors contributing to regional sea-ice variability.

The mean sea-ice conditions in the SIMBA and SIPEX regions are known to be very different (e.g., Gloersen et al., 1992). Mean (1979-2007) September sea ice in the SIMBA region (90-95°W) extends from approximately 64° to 72°S (~890 km north-south), whereas in the SIPEX region (between 115-130°E), it extends from approximately 61.5° to 66.5°S (~560 km north-south). Other

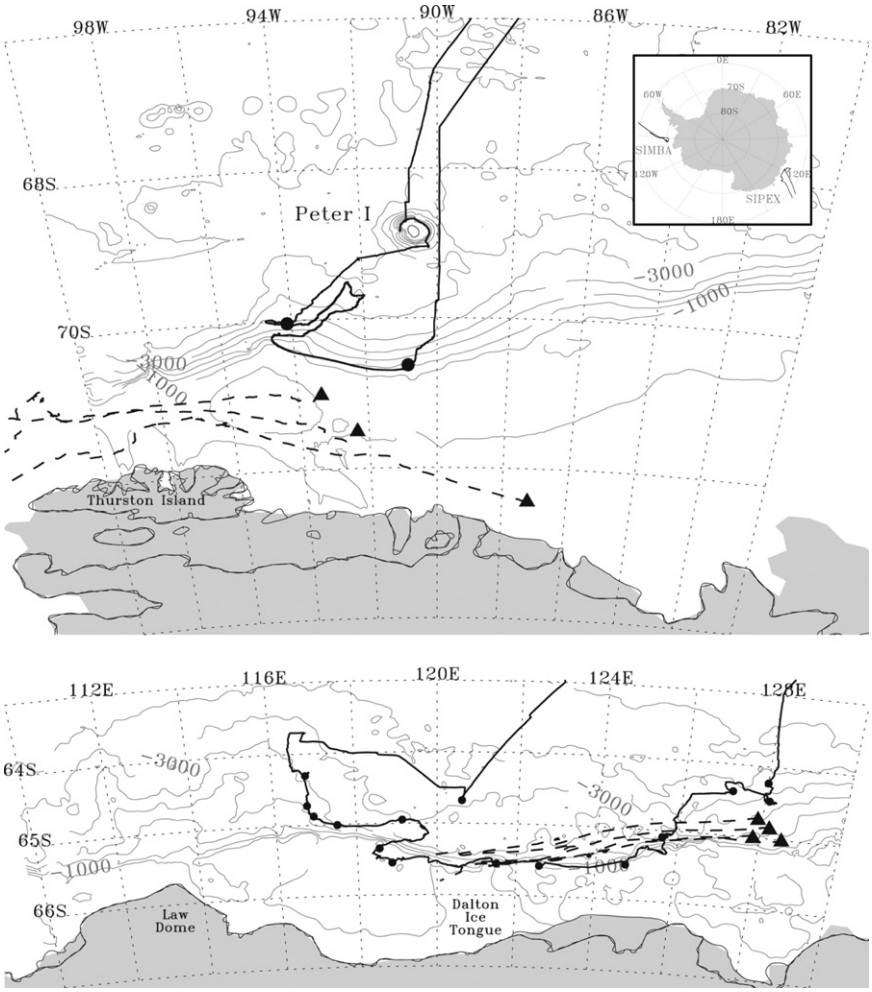

Fig. 1. Maps of the (A) SIMBA and (B) SIPEX cruise tracks (bold lines) and study regions. SIMBA's predominantly westward month-long drift track includes the section between the two black dots, while black dots along SIPEX's westward cruise track demarcate the location of 15 ice stations. Bathymetric contours and land/ice shelves are in grey. Black dashes trace the westward drift tracks of ice buoys: three deployed on summer sea ice prior to SIMBA in March 2007 (Ted Maksym, unpublished data), and four deployed during SIPEX on 12 September 2007 (Heil et al., in press); triangles indicate deployment locations.

differences include greater sea-ice thickness in the SIMBA region (Worby et al., 1996; Worby et al., 2008a) and deeper snow cover (Markus and Cavalieri, 1998; Worby et al., 2008b). Observations also indicate that the deeper snow cover on sea ice in the Bellingshausen Sea results in widespread surface flooding and warmer sea ice, making it the warm 'end-member' of the Antarctic spectrum (Perovich et al., 2004).

SIMBA took place in the western Bellingshausen Sea (here delimited by the Antarctic Peninsula and 100°W). As described by Jacobs and Comiso (1997), this was in an area renowned for its heavy multi-year sea-ice cover and was the region through which the beset *Belgica* drifted westward during 1898-99. Based on the modern satellite sea-ice record, however, the summer sea-ice cover in the southern Bellingshausen Sea showed widespread retreats

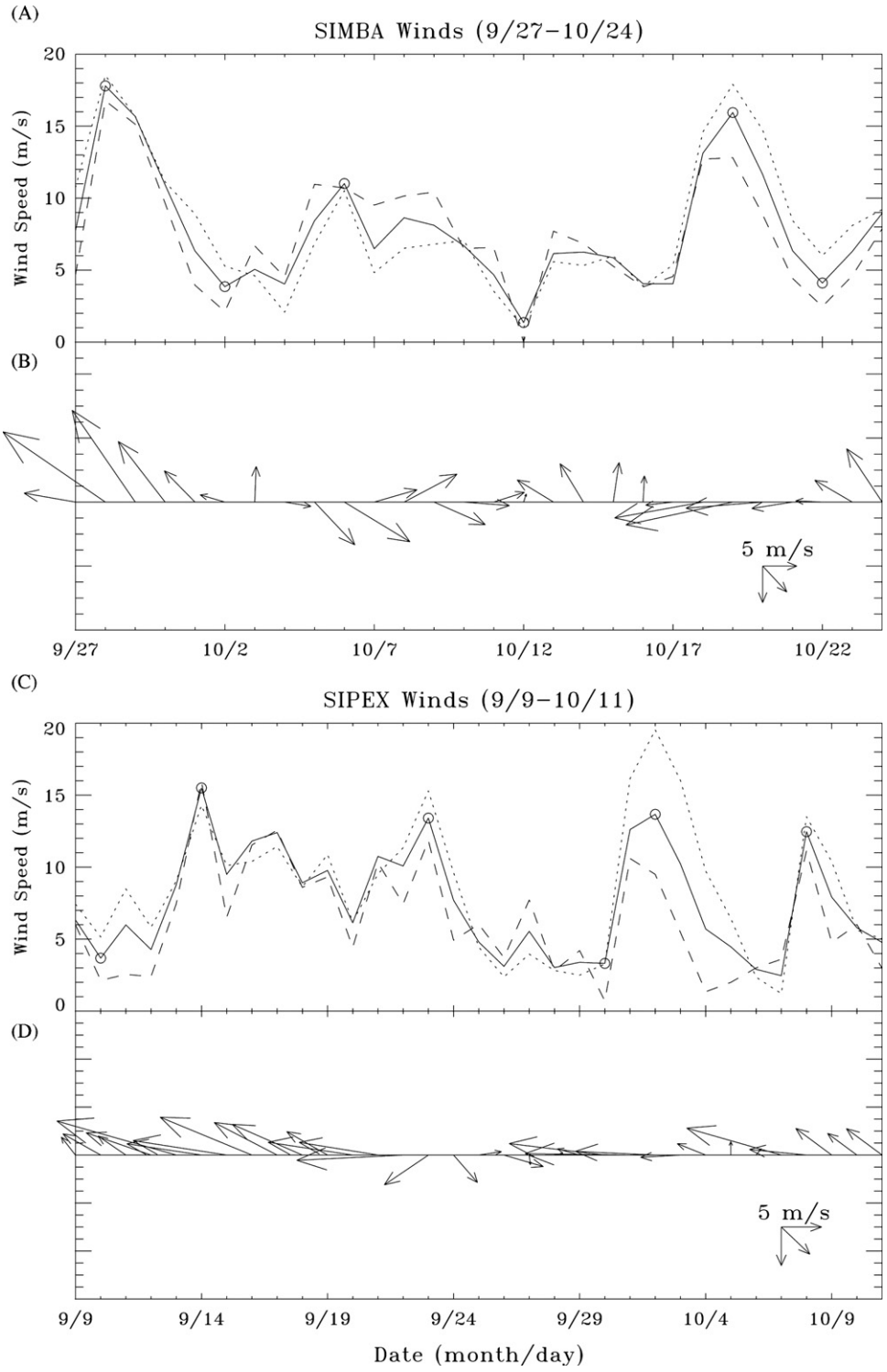

Fig. 2. Daily time series of NNR wind speed and direction for the (A, B) SIMBA and (C, D) SIPEX study regions during the field campaigns. For the SIMBA region, winds were averaged over 68-71°S, 90-95°W (solid curve and vectors) or extracted for 69.5 °S/93.75°W (dashed) and 71.4°S/93.75°W (dotted), respectively. For the SIPEX region, winds were averaged over 63-67°S, 115-130°E (solid curve and vectors) or extracted for 63.8°S/123.75°E (dashed) and 65.7°S/123.75°W (dotted), respectively. Wind direction indicates where winds are blowing to; a left pointing arrow indicates a wind blowing to the west (i.e., an easterly wind).

starting in the late 1980s (Jacobs and Comiso, 1993, 1997; Stammerjohn et al., 2008). These summer sea-ice retreats were associated with strong northerly winds and warm air temperature (Jacobs and Comiso, 1997; Massom et al., 2006; Stammerjohn et al., 2008). Consecutive summers of anomalously low summer sea-ice extent, as was observed for 1989-1992, 1999-2001, 2007-2009, suggest a possible additional influence by the ocean, e.g., weaker surface currents or changes in upwelling of Circumpolar Deep Water (Jacobs and Comiso, 1997). Since the ice-free summer period of 1989-1992, which removed much of the thicker multi-year sea ice from this region (Jacobs and Comiso, 1997), satellite observations of sea ice in the Bellingshausen Sea revealed more advance/retreat episodes during winter (Harangozo, 2004, 2006) and a tendency towards earlier spring sea-ice retreats (Massom et al., 2006; Massom et al., 2008) and later autumn sea ice advances (Stammerjohn et al., 2008). The apparent erosion of perennial sea ice in the southern Bellingshausen Sea will likely affect adjacent regions. Climatological sea-ice drift data indicate that most sea ice produced in the Bellingshausen Sea is exported northward, except for a coastal band (of variable width) that is exported westward to the Amundsen Sea (e.g., Assmann et al., 2005).

In contrast, East Antarctica has little multi-year sea ice, less snow, thinner first-year sea ice (Worby et al., 2008b), and no significant sea-ice trends over 1979-2007 (Comiso and Nishio, 2008). Although relatively narrow, the East Antarctic sea-ice cover, containing the SIPEX study region, comprises a series of recurrent zones, each with distinct physical characteristics that reflect broad-scale climatological patterns of atmospheric and oceanic circulation and temperature (Massom et al., 1999). These zones are similar to those found in the Bellingshausen Sea but occur over shorter distances and comprise (i) a well-developed marginal ice zone; (ii) an inner pack ice zone characterised by more stable conditions, larger floe sizes and thicker snow cover; and (iii) a complex coastal zone characterised by fast ice (Giles et al., 2008) and recurrent latent heat polynyas (Massom et al., 1998). Climatological sea-ice drift south of the Antarctic Divergence is predominantly westward within the Antarctic Coastal Current, while that in the north is more to the east, with a northward retroflection within the Prydz Bay Gyre (Heil and Allison, 1999). In summer, sea-ice retreats to the coast in most of this sector (Gloersen et al., 1992).

2. Data

To assess the regional and circumpolar ice-atmosphere-ocean conditions during IPY 2007, we use satellite-derived and numerically-analyzed surface and atmospheric variables. These include sea-ice extent, concentration, duration and motion, sea-surface temperature, sea-level pressure, surface winds, cyclone density, precipitation and snow accumulation.

Sea-ice concentration (SIC) and extent (SIE) for 1979-2007 are from Version 2 of the Goddard Space Flight Center (GSFC) Bootstrap Scanning Multi-channel Microwave Radiometer-Special Sensor Microwave/Imager (SMMR-SSM/I) daily and monthly time series (Comiso, 1999), augmented with Near Real Time Sea Ice daily data for 2008 (Maslanik and Stroeve, 1999) (the latter are for qualitative purposes only and not included in statistical analyses). Maps of sea-ice advance and retreat are derived from the daily data by tracking the ice edge through space and time (see Stammerjohn et al., 2008). Ice season duration, and summer open-water duration, are

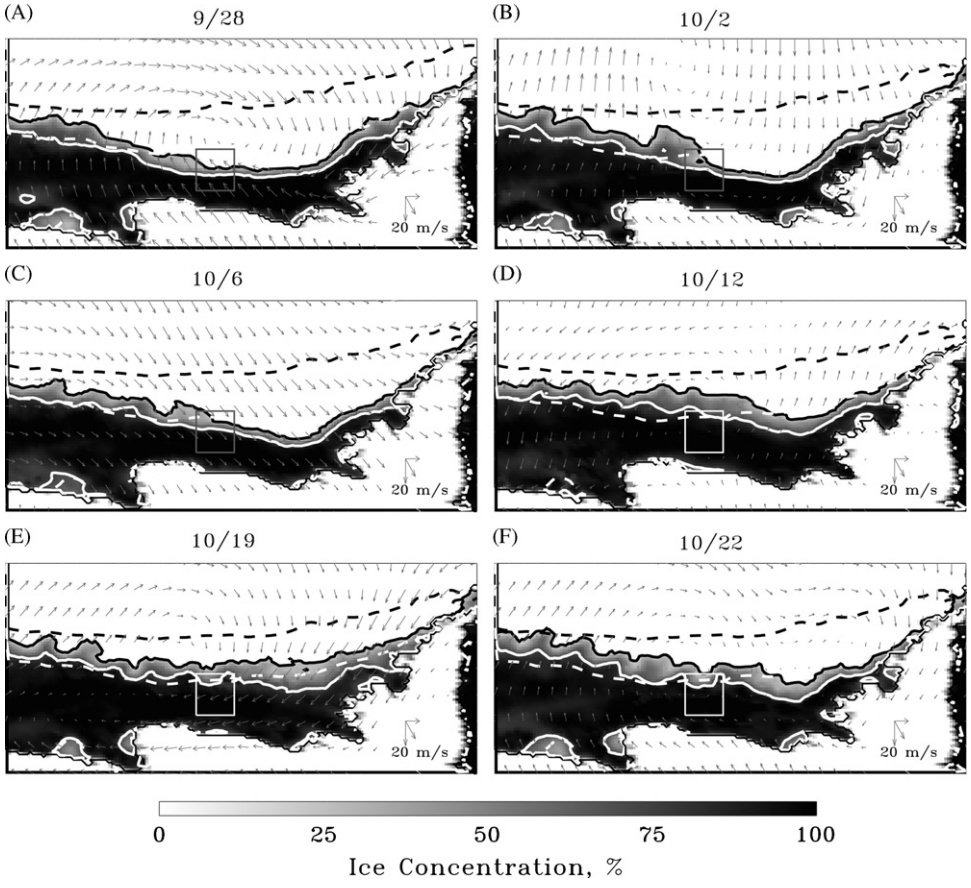

Fig. 3. Daily snapshots of SMMR-SSM/I sea-ice concentration and NNR winds for the greater SIMBA region (60.5°S-75.2°S, 58°W-120°W). The boxed area corresponds to the study region (68-71°S, 90-95°W), and the solid black and white contours outline the 15% (i.e., ice edge) and 75% ice concentration contours, respectively. The dashed black and white contours show the 1979-2007 monthly means for either September (A) or October (B-F).

determined from the time elapsed between day of advance and subsequent retreat, and day of retreat and subsequent advance, respectively.

Sea-surface temperature (SST) fields are from the NOAA OI.v2 monthly SST analysis derived from the optimum interpolation (OI) version 2 fields (Reynolds et al., 2002). Numerically analyzed data of sea-level pressure (SLP) and 10-m winds are from the National Center of Environmental Prediction (NCEP) and National Center for Atmospheric Research (NCAR) Reanalysis (NNR) Project (Kalnay et al., 1996) and are used to infer monthly to seasonal changes in regional storm activity. We use these data from 1979 onwards, when the introduction of satellite data into the numerical data analysis in late 1978 led to a marked improvement in the NNR data for the Southern Ocean.

Cyclone density anomaly fields were derived from 6-hourly mean sea-level pressure of NCEP-2 reanalysis (1979 – current) using the University of Melbourne's Automatic Cyclone Tracker (Murray and Simmonds, 1991). The cyclone tracker uses a search window for local maxima in the surface pressure relative to the neighboring grid points. The location of a pressure minimum is sought iteratively from the local maxima using ellipsoidal minimization techniques. Only pressure systems that satisfy the minimum concavity criterion (Simmonds, 2003), which ensures that they are of meteorological significance, are considered in this analysis.

Precipitation was derived from the European Centre for Medium range Weather Forecasts (ECMWF) interim reanalysis. Although we used NNR for SLP and 10-m winds and NCEP-2 for cyclone density, ECMWF-derived precipitation was preferred, since it compares reasonably well with available field data (Leonard and Cullather, 2008; Marshall, 2009) as described below and is less prone to spurious wave patterns that would greatly affect regional estimates (Cullather et al., 1998). There is less convincing evidence that NNR-derived precipitation data compare as well. In contrast, ECMWF- and NNR-derived SLP and 10-m winds are similar (e.g., Bromwich et al., 2007), but we chose to use the NNR-derived data, because NNR provides a longer time series (here starting in 1979) and facilitates comparison with other relevant studies (e.g., Stammerjohn et al., 2008; Vancoppenolle et al., 2011).

Qualitative comparisons of monthly mean ECMWF precipitation against precipitation reports from three Antarctic bases reveal that the re-analysis successfully captured the seasonal cycle of precipitation at these coastal sites (Marshall, 2009). Over Antarctic sea ice, the accuracy of precipitation analyses is not well known, as there are few accumulation data to validate the reanalysis data. However, Leonard and Cullather (2008) showed that there was reasonable correspondence between precipitation events from the ECMWF operational forecasts and ship-based measurements in the Bellingshausen Sea. Despite possible limitations in the spatial distribution of snowfall (Maksym and Markus, 2008), this suggests that the ECMWF reanalysis is at least capable of resolving qualitative inter-annual variations in precipitation. To avoid forecast errors due to model spin-up, the daily average precipitation was determined as in Marshall (2009). We used precipitation rather than P-E as evaporation will dominate over leads and other open water areas. No correction was made to exclude liquid precipitation. This may be a significant portion of total precipitation close to the ice edge at lower latitudes (Sturm et al., 1998).

Snow depth was estimated from Special Sensor Microwave/Imager (SSM/I) brightness temperatures using the algorithm of

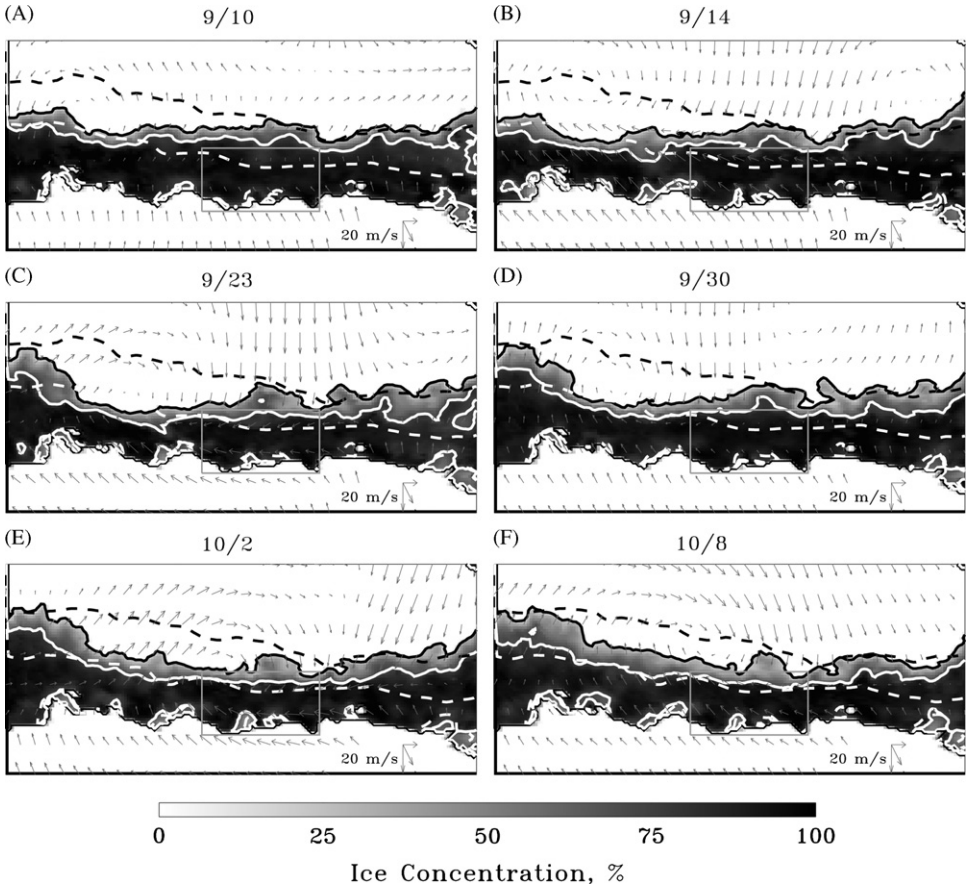

Fig. 4. Daily snapshots of SMMR-SSM/I sea-ice concentration and NNR winds for the greater SIPEX region (56.2°S-69.5°S, 90°E-150°E). The boxed area corresponds to the study region (63-67°S, 115-130°E), and the solid black and white contours outline the 15% (i.e. ice edge) and 75% ice concentration contours, respectively. The dashed black and white contours show the 1979-2007 monthly means for either September (A-D) or October (E-F).

Markus and Cavalieri (1998), modified for use with bootstrap sea-ice concentrations (Comiso and Nishio, 2008) as described in Maksym and Markus (2008). The algorithm was updated by calibrating it against observed snow depths from the full ASPeCt dataset (Worby et al., 2008a). Compared with the original algorithm, snow depths tend to be on average about 2 cm lower. For analyzing snow depth anomalies as in this paper, the differences are negligible. Since the SSM/I footprint of approximately 625 km^2 integrates over flat and ridged areas of individual floes, the snow-depth product must be regarded as an areal averaged estimate. Passive microwave snow depth is prone to errors due to snow properties (Markus and Cavalieri, 2006) and deformed sea ice (Worby et al., 2008b). Despite these limitations, the dataset appears to capture some features of regional and interannual variability (Maksym and Markus, 2008; Markus et al., 2006). This suggests that interannual variations in snow depth are qualitatively discernable in the satellite-derived dataset. For comparison with snow depth, we also derived the potential total snow accumulation on sea ice. For this, precipitation accumulated over several months prior to the field experiments was computed, but only where sea ice was present in a given month, so that the precipitation over open-ocean was excluded. This is a maximum potential accumulation, as it does not account for reductions in mean snow depth due to sea-ice divergence, blowing snow, or snow-ice formation.

Information on regional scale sea-ice motion is derived from satellite passive microwave brightness temperature data (Fowler, 2003). Daily gridded fields were obtained from the US National Snow and Ice Data Center (http://nsidc.org/data/nsidc-0116.html) at a spatial resolution of 25 by 25 km. We also show the drifting satellite-tracked buoys deployed prior to SIMBA (Fig. 1A, Maksym, unpublished data) and during SIPEX (Fig. 1B, for full analysis, see Heil et al., in press).

3. Results

We begin our assessment of regional sea-ice conditions in the SIMBA and SIPEX regions by examining the daily sea-ice and wind conditions during the time of the field campaigns (September-October 2007). We next examine the regional monthly conditions leading up to and during the field campaign, starting with May, which captures anomalies associated with the sea-ice advance, and ending with October. Over both the daily and monthly time scales we investigate the general correspondence between regional winds, sea-ice extent and drift. The regional analysis is then placed into the context of circumpolar variability, where 2007 monthly (May-October) anomalies in SST, SLP and SIC (with respect to 1979-2007) are presented for evaluating the simultaneous occurrence of ice-atmosphere-ocean surface anomalies. We conclude with an examination of anomalies in the timing of the 2007 sea-ice advance and subsequent retreat in relation to storm density, precipitation and snow depth to characterize the regional distribution of snow on sea ice.

3.1. Daily Winds and Sea-Ice Conditions during SIMBA and SIPEX

Time series of daily wind speed and direction for both study regions (Fig. 2) highlight high- and low-wind days (open circles in Fig. 2A and C) for which we show the regional wind and sea-ice conditions (Figs. 3 and 4). Detailed studies of daily meteorological

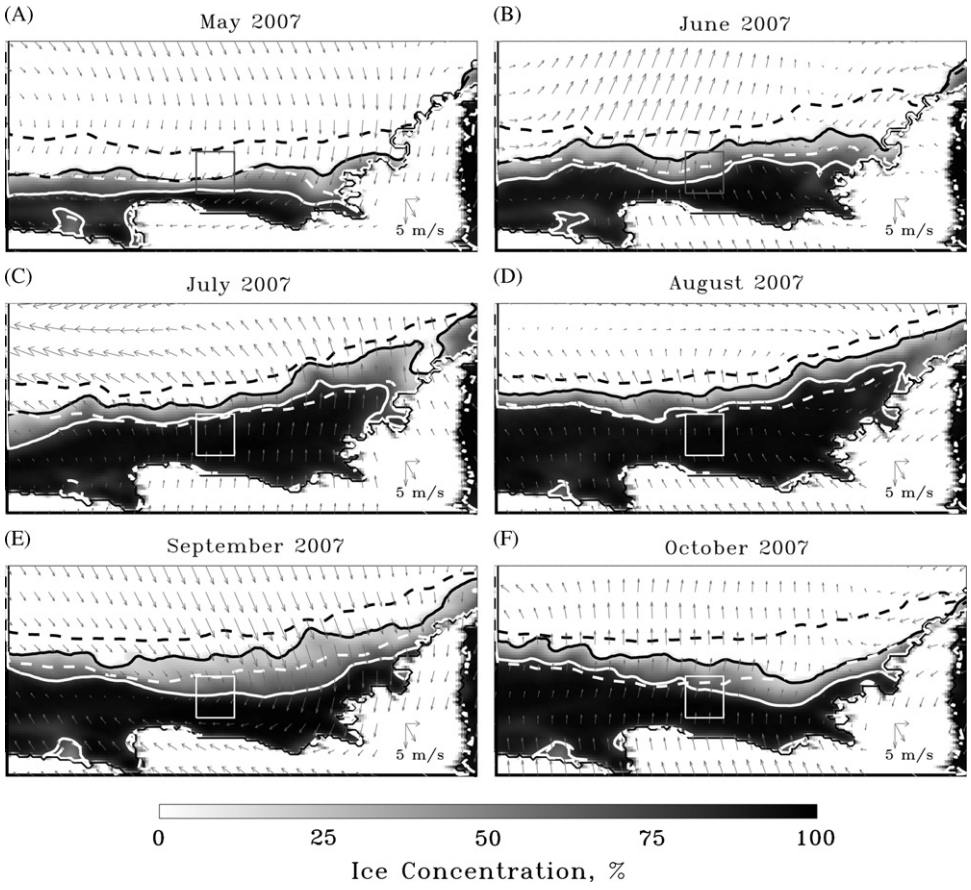

Fig. 5. May-October 2007 (A-F) monthly means of SMMR-SSM/I sea-ice concentration and NNR monthly wind anomalies (based on 1980-2007) for the greater SIMBA region. Regions and solid/dashed contours defined as in Fig. 2A but for the months May-October.

conditions at the field sites and the corresponding snow and sea-ice conditions are featured elsewhere (Leonard and Cullather, 2008; Lewis et al., 2011; Vancoppenolle et al., 2011; Worby et al., in press; Xie et al., 2011). Here we are interested in the general correspondence between daily regional winds and sea-ice extent changes that led to strong and weak surface forcing events while SIMBA and SIPEX were underway.

Six daily snapshots of regional wind and sea-ice conditions during SIMBA (Fig. 3) show large negative ice-edge anomalies, particularly east of SIMBA where northerly winds prevailed. In spite of this anomalously early spring sea-ice retreat, there was a short period of ice edge advance between October 7-17, again largely to the east of SIMBA and during a time of weaker winds with a more southerly component in that area. At the SIMBA study site, sea-ice concentrations were near 100% and drift was largely unconstrained (in free drift). Changes in ship drift track (Fig. 1A) followed these quasi-weekly changes in wind directions (Fig. 2B), e.g., with initial drift to the west/northwestward during south-easterly winds, followed by eastward drift during northwesterly winds, and northeastward during westerly winds, and so on.

Six daily snapshots of regional wind and sea-ice conditions during the SIPEX campaign (Fig. 4) show large negative ice-edge anomalies northwest of SIPEX but heavier pack ice conditions within and east of SIPEX (i.e. the 75% sea-ice concentration contour was north of its mean monthly position). Sea-ice conditions did not appear to change substantially over this time period, though west of SIPEX (near the plotted edge at 90°E), there was an ice edge advance due to persistent southerly winds. There was some

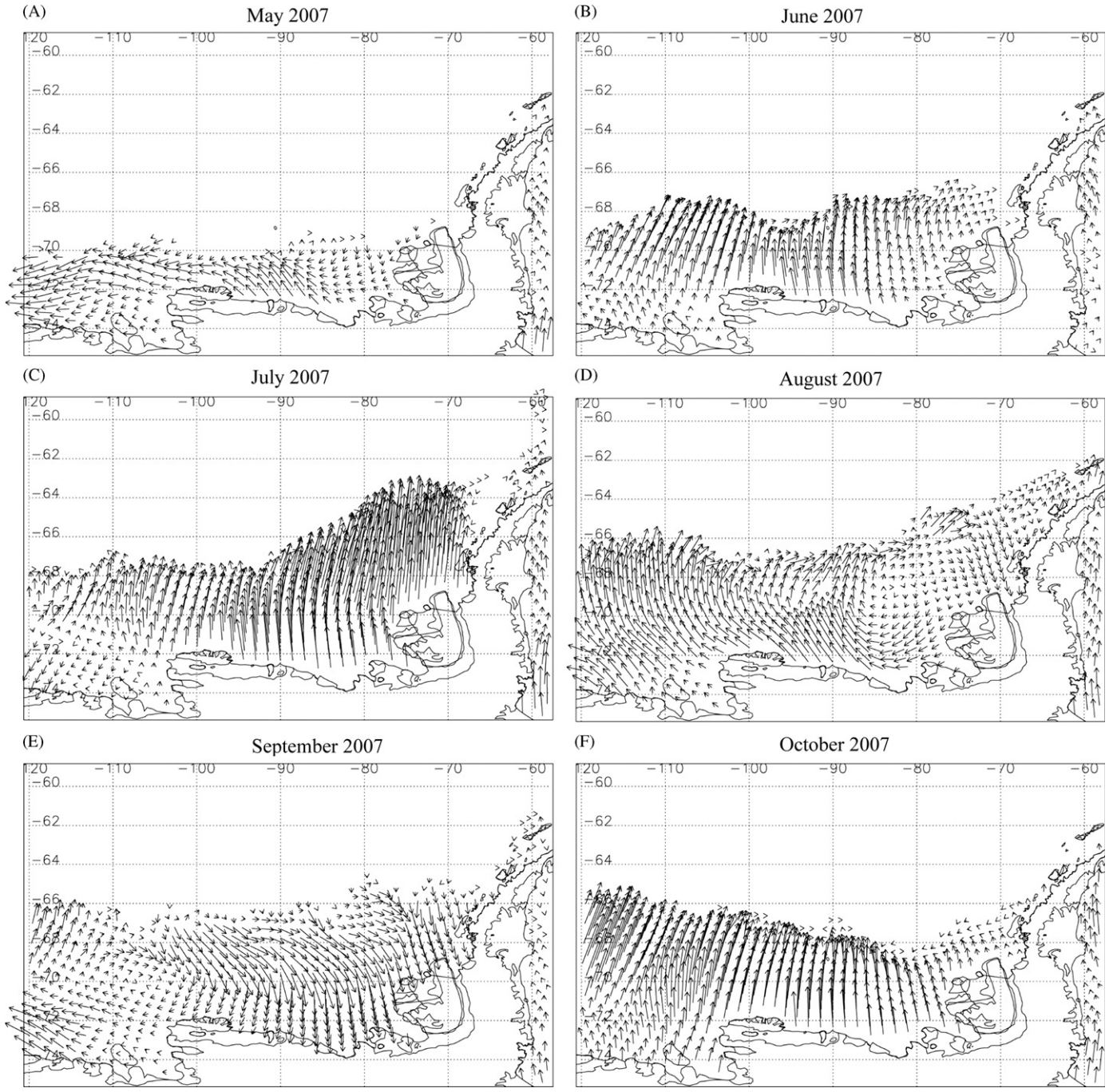

Fig. 6. May-October 2007 (A-F) monthly means of SSM/I sea-ice motion for the greater SIMBA region (as defined in Fig. 2). See Fig. 8 for drift speed legend.

ice-edge retreat to the northwest of SIPEX between September 14 and 23 (associated with northerly winds), but the ice edge appeared to recover (re-advance) with more southerly winds after September 23. Within the SIPEX region, winds were mostly easterly to southeasterly over the study period (Fig. 2D), and together with the prevailing westward coastal current, lead to westward sea-ice drift as indicated by buoys deployed on September 12 in the eastern SIPEX region (Fig. 1B, Heil et al., in press).

3.2. *Monthly Winds, Sea Ice and Drift Conditions Leading up to SIMBA and SIPEX*

Monthly-averaged sea-ice concentrations from May to October for the greater SIMBA region (Fig. 5) show negative ice-edge anomalies (i.e., the 15% sea-ice concentration contour is south of the monthly mean) in all months leading up to and during SIMBA. Monthly wind anomalies are also shown and correspond well with sea-ice extent changes, particularly for the inner pack-ice region as highlighted by the 75% sea-ice concentration contour. In contrast to ice-edge extent, the inner pack-ice extent shows region-wide negative extent anomalies in May (in association with northerly winds), but near average extent from June to August (in association with southerly winds). In September, negative ice-edge and inner pack-ice-extent anomalies appear again (in association with strong northerly winds), particularly within and east of the SIMBA study area, and in October the west-east contrast persists with less pronounced negative ice-edge anomalies in the west due to southerly winds in that sector.

Monthly-averaged sea-ice motion for the greater SIMBA region (Fig. 6) corresponds closely with monthly averaged wind anomalies. The large negative ice-edge anomalies in May (Fig. 5A) were associated with south and westward ice drift and the export of sea ice from the Bellingshausen Sea to the Amundsen Sea. With mostly southerly winds from June to August, sea-ice drift was northward and assisted the late advance of the ice edge north of the SIMBA region. That ice-edge advance was partially reversed by strong northerly winds in September, which caused southward drift within and east of the SIMBA region, only to be reversed again in October with strong northward drift within and west of the SIMBA region. Overall, there was net northward sea-ice drift over the May-October 2007 time period. In spite of this, the ice edge remained south of its mean location. As will be shown below, SSTs were anomalously warm equatorward of the pack ice and likely contributed to the negative ice-edge anomaly. Compared to mean (1988 to 2007) ice-drift rates, drift anomalies in the SIMBA region during 2007 (not shown) were marked by higher than usual westward motion, while to the west of SIMBA an increased north-eastward flow was observed. Together they resulted in greater-than-average cyclonic ice motion in the region.

Monthly-averaged winds and sea ice for the greater SIPEX region (Fig. 7) show negative ice-edge (and inner pack ice extent) anomalies to the north and west of SIPEX from May to October, largely associated with northerly wind anomalies in May, July and September (with weaker wind anomalies in June and August). However, of particular note is the northward sea-ice drift in August in the area of 105-115°E (Fig. 8D) that failed to advance the ice edge in this region (Fig. 7). Similar to SIMBA, SSTs were anomalously warm equatorward of the pack ice and may explain the persistent negative ice-edge anomaly in this area. However, in the far west (near 90°E), the ice edge did eventually reach its mean location in October (Fig. 7F) in association with overall stronger southerly winds and

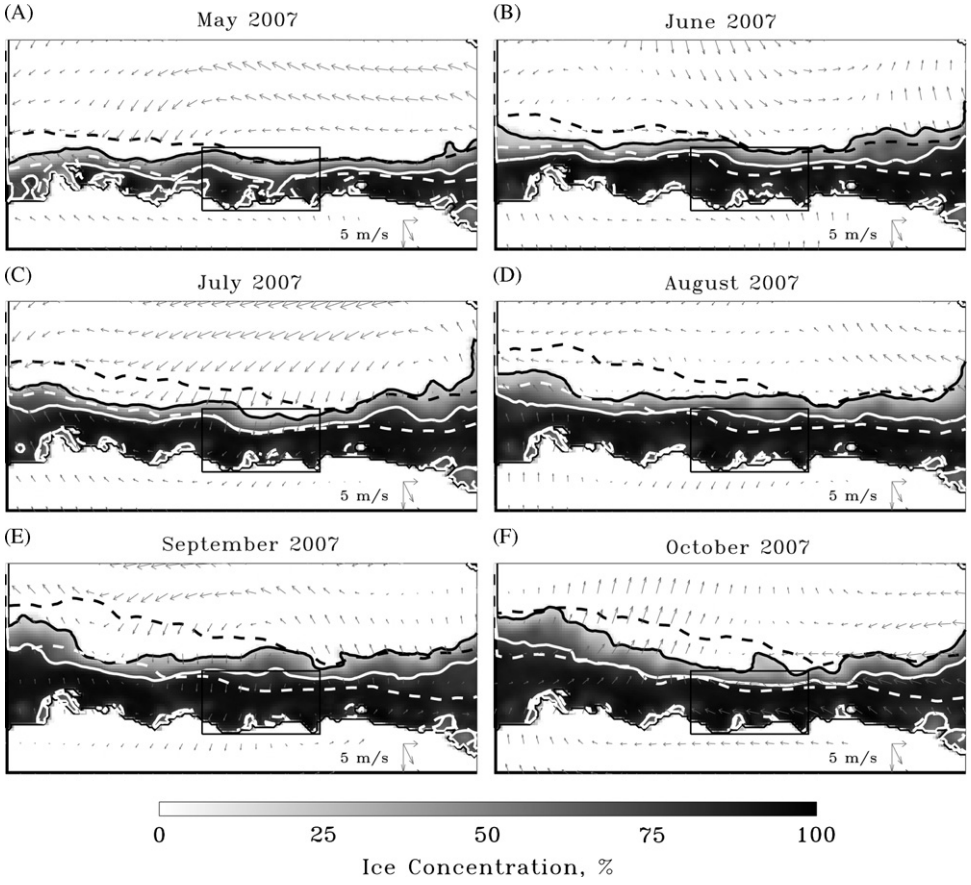

Fig. 7. May-October 2007 (A-F) monthly means of SMMR-SSM/I sea-ice concentration and NNR monthly wind anomalies (based on 1980-2007) for the greater SIPEX region. Regions and solid/dashed contours defined as in Fig. 2B but for the months May-October.

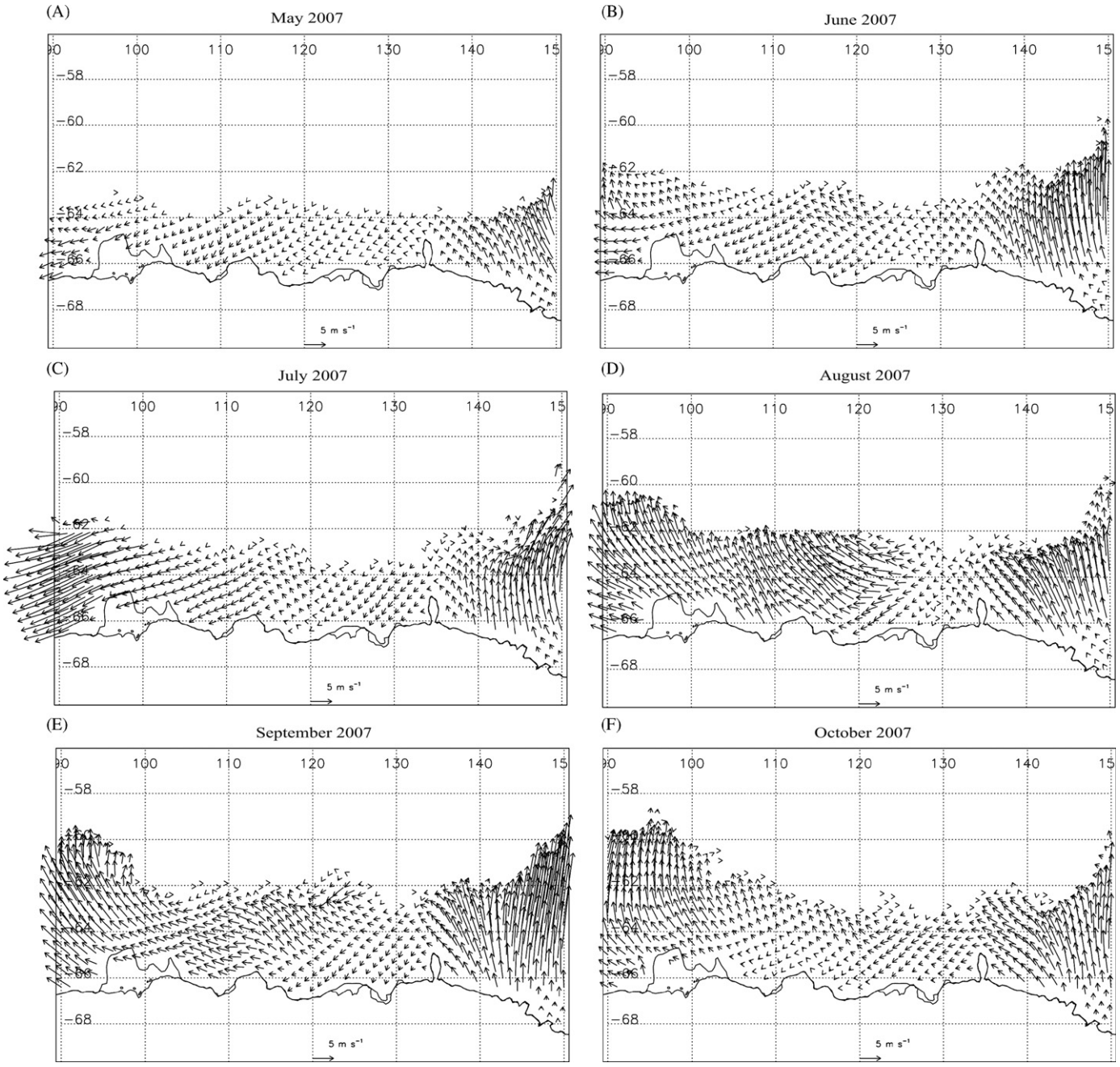

Fig. 8. May-October 2007 (A-F) monthly means of SSM/I sea-ice motion for the greater SIPEX region (as defined in Fig. 2).

northward sea-ice drift from August to October (Fig. 8 D-F). In contrast, to the east of SIPEX (130-140°E), ice edge and inner pack-ice extent anomalies were mostly equatorward of the mean from May to October in association with southerly wind anomalies (Fig. 7), northward sea-ice drift (Fig. 8), and as will be shown below, cool SSTs equatorward of the pack ice.

Within the SIPEX region, wind anomalies were weak and mostly easterly in May and June (though difficult to see in Fig. 7 A-B given the short vector lengths), and sea-ice drift was slow and westward (Fig. 8 A-B), following the coastal current (Heil et al., in press). From July to September, wind anomalies became moderate and north-easterly (Fig. 7 C-E), and the westward sea-ice drift strengthened (Fig. 8 C-D). In October, and despite moderate easterly winds (Fig. 7F), westward sea-ice drift slowed relative to the preceding three months (Fig. 8F). Compared to the overall SSM/I record (not shown), the SIPEX region experienced an increased westward flow in 2007, while the eastern SIPEX area was marked by higher northward ice motion. Thus, in contrast to the strong northerly winds and southward sea-ice drift during September in the SIMBA region (Figs. 5 and 6E), the SIPEX region experienced relatively mild wind conditions and moderate but persistent westward sea-ice drift (Figs. 7 and 8E).

To summarize the sea-ice extent changes and to show how year 2007 compared to the 1979-2008 satellite record, time series of regionally-averaged sea-ice extent for the greater SIMBA and SIPEX regions is shown in Fig. 9. For both regions, monthly sea-ice extent was below average for most months (Fig. 9A, Table 1). The low annual sea-ice extent in the SIMBA region in 2007 (Fig. 9B) follows the overall downward trend observed in this area (Comiso and Nishio, 2008) (Table 2), with the following year (2008) being the lowest year yet observed. In contrast, the SIPEX region shows a weak positive trend in annual sea-ice extent (Fig. 9B), but with

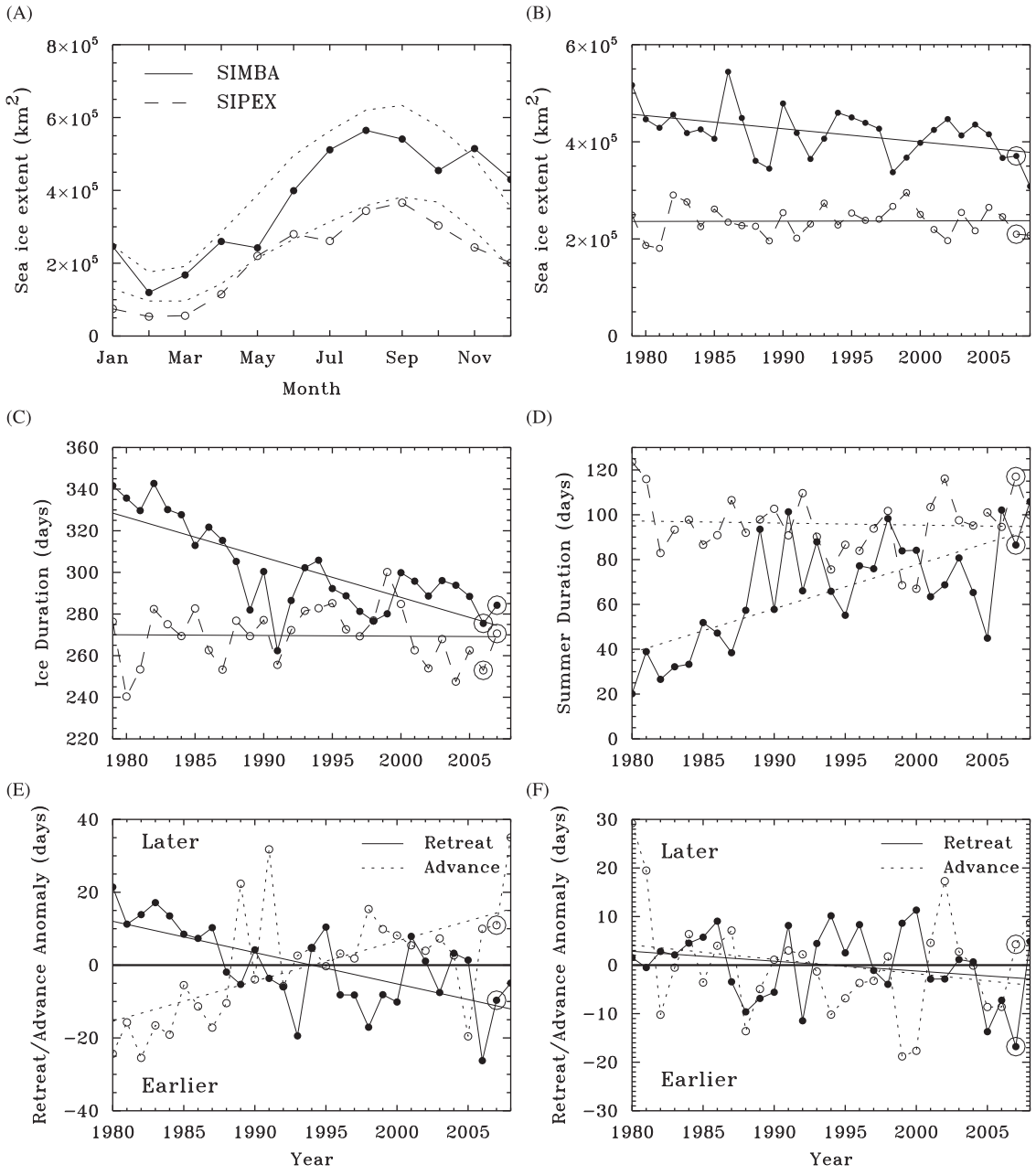

Fig. 9. Time series of SIMBA (68-71°S, 85-100°W) and SIPEX (63-71°S, 115-130°E) regional averages of (A) 2007 monthly sea-ice extent (km^2) (dotted curves show 1979-2007 mean annual cycle), (B) 1979-2007 annually (January-December) averaged sea-ice extent (km^2), (C) 1979-2007 ice season duration (days), (D) 1979-80 to 2007-08 open water duration (days), and (E) SIMBA and (F) SIPEX 1979-80 to 2007-08 anomalies in the timing of sea ice retreat and subsequent advance (in days). Trend lines are shown for (B-F).

2007 and 2008 as negative departures. (The other sea-ice time series in Fig. 9 C-F will be discussed further below.)

3.3. *Circumpolar Distributions of Ice-Ocean-Atmosphere Anomalies in 2007*

We now place the regional sea-ice studies into a circumpolar context relative to mean (1979-2007) conditions by analyzing monthly anomaly maps of SIC, SST and SLP (Fig. 10). We then examine circumpolar anomalies in the timing of autumn sea-ice advance, spring retreat and resulting ice-season duration (Fig. 11).

From May to October, the SIMBA and western SIPEX regions show negative SIC anomalies with warm SSTs equatorward of the ice edge (Fig. 10). Elsewhere, the SIC anomalies are mostly positive and SST's are cool south of 55°S. The spatial extent of the low SIC/warm SST anomalies in the southeast Pacific extends well beyond the SIMBA region and includes the entire Bellingshausen and Amundsen seas (60-130°W) for all months except October, though high SIC anomalies appear along the coast in July-August in the Bellingshausen and Amundsen seas. Similarly, and west of SIPEX, the low SIC/warm SST anomalies extend to 80°E, though starting in July there is a westward expansion of positive SIC anomalies along the coast into this region. The regional pattern of warm SSTs in the greater SIMBA and SIPEX regions, with cooler SSTs particularly in the Ross and western Weddell seas, was still evident in December (not shown) though with decreased spatial extent and magnitude.

The negative ice-edge anomalies (Figs. 5 and 6) and low SIC in the SIMBA and western SIPEX region from May to September are consistent with the anomaly observed in the timing of sea-ice advance (Fig. 11A, see also Stammerjohn et al., 2008). In both regions, sea-ice advance was late, by up to 2 months in some areas

Table 1
Summary of various sea-ice variables for the SIMBA (68-72°S, 85-100°W) and SIPEX (63-67°S, 115-130°W) regions for year 2007 as compared to the 1979-2007 mean (in parentheses). Sea-ice extent is the area inside the ice edge as defined by the 15% sea ice concentration contour. Annual sea-ice extent is calculated from monthly averages and is based on the calendar year (January-December). Sea-ice advance and retreat are determined from daily sea-ice extent time series (for each imaged pixel) and are based on the seasonal sea-ice year that begins and ends during the mean summer minimum (i.e., starting on year day 46, February 15, and ending on year day 410, February 14 of following year). Ice season duration is the time (in days) between the autumn advance and subsequent spring retreat. Conversely, the summer open water (OW) period is the time between the spring retreat and subsequent autumn advance.

Sea Ice Variable	SIMBA	SIPEX
2007 Annual SIE (km^2)	370895 (421285)	209812 (237787)
2007 September SIE (km^2)	540896 (638635)	366139 (384214)
2007 October SIE (km^2)	454534 (582078)	303441 (369348)
2006-07 Retreat (day)	373 (1/8) [383 (1/18)]	353 (12/19) [370 (1/5)]
2007 Summer OW (days)	87 (65)	117 (96)
2007 Advance (day)	94 (4/4) [81 (3/22)]	105 (4/15) [101 (4/11)]
2007-08 Retreat (day)	377 (1/12) [383 (1/18)]	375 (1/10) [370 (1/5)]
2007-08 Ice Season (days)	284 (302)	271 (270)

Table 2
SIMBA and SIPEX regional sea-ice trends over 1979-2007.

	SIMBA	SIPEX
Annual extent (km^2/yr)	-2186 ± 1134 ($p=0.03$)	$+277 \pm 686$ ($p=0.35$)
Ice duration (days/yr)	-2.00 ± 0.64 ($p<0.01$)	-0.05 ± 0.44 ($p=0.46$)
Sea ice advance (days/yr)	$+0.99 \pm 0.31$ ($p<0.01$)	-0.40 ± 0.28 ($p=0.09$)
Sea ice retreat (days/yr)	-0.92 ± 0.25 ($p<0.001$)	-0.26 ± 0.21 ($p=0.12$)
Summer open water (days/yr)	$+1.90 \pm 0.51$ ($p<0.001$)	-0.13 ± 0.41 ($p=0.37$)

compared to the mean, while in the eastern SIPEX region sea-ice advance was early. The subsequent sea ice retreat anomaly map (Fig. 11B) shows weaker anomalies in these two regions and more spatial variability overall. East of SIMBA, sea-ice retreat was early but north and west of SIMBA it was average to late due to the noted changes in October, i.e. the southerly winds and northward sea-ice drift (Figs. 5 and 6F). In the SIPEX region, sea-ice retreat was late in the coastal region but early offshore. The resulting ice season duration map (Fig. 11C) reflects the strong anomalies in sea-ice advance, showing shorter-than-average ice-season duration in the SIMBA and western SIPEX regions, particularly east of SIMBA and west of SIPEX where the duration was up to 3 months shorter.

Within the SIMBA study area, the 2007 advance was 13 days later, and the retreat 6 days earlier, compared to the mean (Table 1). As with annual sea-ice extent, the short ice-season duration in year 2007 (Table 2) was a continuation of downward sea-ice trends in this region (-2 days/year, Stammerjohn et al., 2008), such that ice-season duration was about 58 days shorter in 2006-07 (and 2007-08) than it was in 1979. In the SIPEX region, because of the east-west differences (which average out), the 2007 advance, retreat and duration anomalies are fairly weak (Tables 1 and 2, and Figs. 9C and 11D).

In both the SIMBA and SIPEX regions, the late sea-ice advance followed an unusually long ice-free summer period (Fig. 9D). The onset of the ice-free summer period is determined by the preceding spring sea-ice retreat (in 2006-07), which was early in both the SIMBA and SIPEX regions (Figs. 9E and 9F, Table 1) and in fact was the earliest yet observed in the SIPEX region (since 1979), contributing to the 2nd longest ice-free summer observed there (Fig. 9D). Further, the regions of warm SSTs were just offshore of the regions showing early 2006-07 sea-ice retreat (not shown) and late 2007 sea-ice advance (Fig. 11A), i.e. between 80°-120°E (including the western SIPEX region) and 80°-140°W (including the SIMBA region), and to a lesser degree between 30°-60°E as well. The map of May SST anomalies (Fig. 10A) shows that the warm SSTs extended well northward of the ice edge and likely resulted from meridional advection of heat associated with the regional atmospheric circulation anomalies (i.e. the wave-3 pattern evident in Fig. 11A). Increased solar ocean warming is expected to have occurred in those areas that had anomalously long ice-free summers, including the SIMBA and SIPEX regions, and as mentioned above, likely contributed to the delays in sea-ice advance.

3.4. Circumpolar Distributions of Cyclones, Precipitation and Snow Depth on Sea Ice in 2007

The annual cyclone density for 2007 (Fig. 12) shows positive anomalies in both the eastern Bellingshausen Sea (60°-90°W) and SIPEX regions (110°-130°E), as well as in the northwestern Ross Sea (70°S, 160°E-170°W) and the southern Weddell Sea (75°S, 30°W). Combining this picture of greater-than-average storm forcing in both the SIMBA and SIPEX regions with the previously discussed sea-ice conditions, we now turn to monthly precipitation and snow-depth anomalies.

To examine the role of snowfall and accumulation on sea-ice conditions before and during the field experiments, we compare ECMWF estimates of precipitation with satellite passive microwave snow depth. In the SIMBA region, precipitation was anomalously high (relative to the 1989-2007 mean) in May (Fig. 13A), consistent with the observed stormy conditions (Fig. 10A) and northerly winds (Fig. 5A). However, this coincided with anomalously low sea-ice extent, so much of this precipitation fell on open water. Precipitation in July and August was anomalously low, so the total snowfall on ice in the western Bellingshausen during the 2007 austral winter was low (Fig. 14A). This suggests that snow ice formation prior to SIMBA *may* have been minimal. Heavy snowfall during September (Fig. 13E), consistent with the broad low-pressure anomaly across the region (Fig. 10E), nearly doubled the amount of snowfall available for accumulation at the SIMBA study site (i.e. Fig. 14A vs. 14B).

Any thin ice receiving such heavy snowfall during September would have been susceptible to flooding, unless winds redistributed unconsolidated snow from areas of thin sea ice to thicker more ridged (deformed) sea ice, as observed during the drift experiment (Leonard and Cullather, 2008; Lewis et al., in press). Snow depths observed at the beginning of the SIMBA drift experiment (29 September) were strongly influenced by a storm that preceded initial measurements on the ice floe (maximum hourly wind speeds of 30 m/s on 27 September, Vancoppenolle et al., 2011). Sustained high and directionally consistent winds could easily have eroded most available snow from level ice regions and deposited it in the lee of ridges and into leads. Similar wind-driven redistribution was regularly observed following weaker storms during the course of the drift experiment, leading to low accumulation recorded by Ice Mass Balance buoys on level ice, while much higher values were measured in ridged areas (Lewis et al., 2011).

In the East Antarctic sector, precipitation anomalies leading up to the field campaigns were zero to negative, with the exception being the positive anomalies in the greater western SIPEX region 90°-120°E (Fig. 13). The stormiest month in 2007 in the SIPEX region (based on pressure anomalies) was May (Fig. 10A), corresponding with the most positive precipitation anomaly in the western SIPEX area. Because sea-ice extent was anomalously low in the SIPEX region in May, much of this precipitation also fell on open

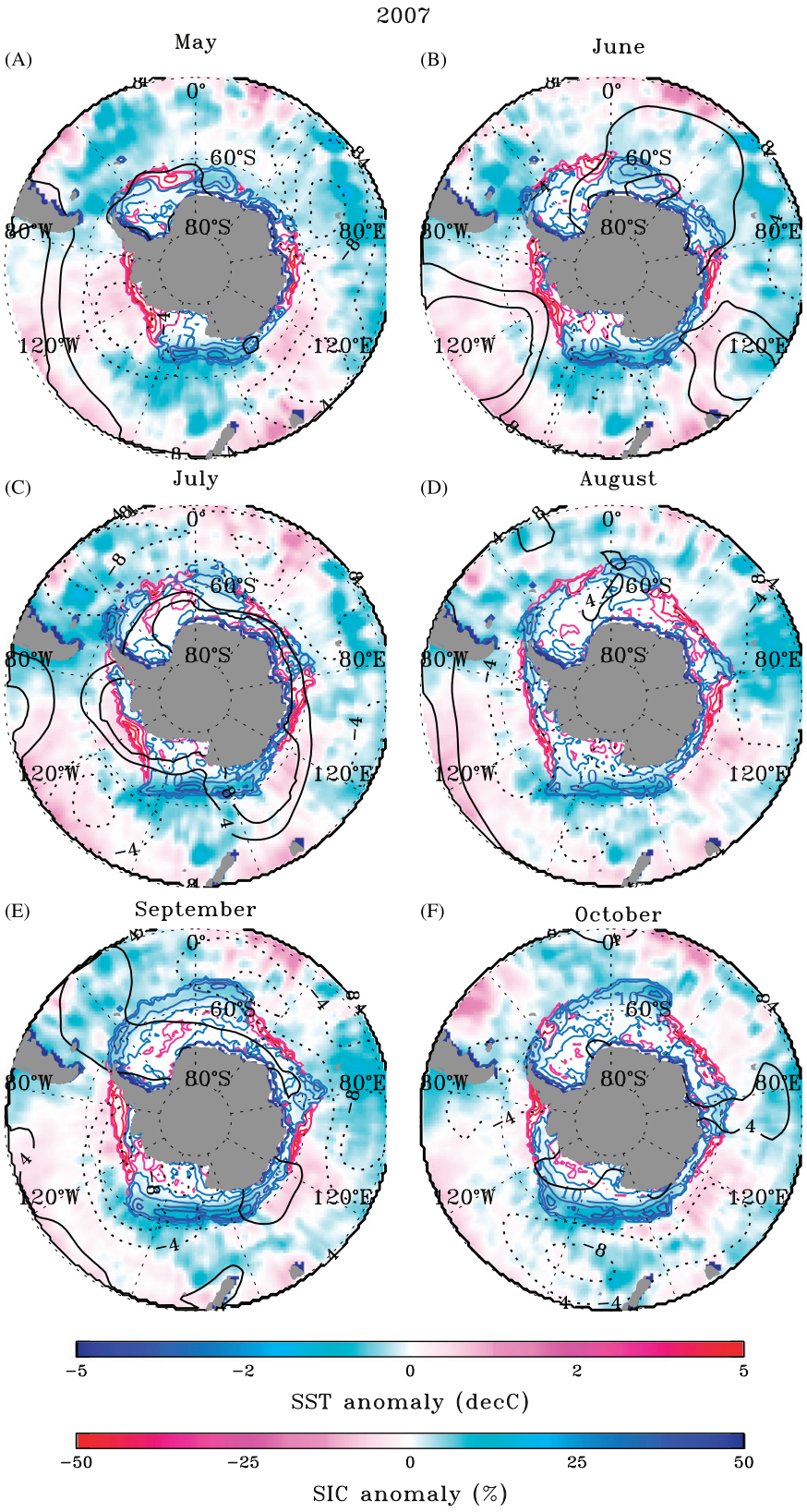

Fig. 10. May-October 2007 circumpolar monthly anomalies (based on 1979-2007) of Reynolds sea-surface temperature (SST) in color shading, SMMR-SSM/I sea ice concentration (color contours) and NNR sea-level pressure (black contours, dotted negative, solid positive).

water. Despite this, the consistently positive precipitation anomalies throughout winter and into spring led to high potential accumulation rates in the western SIPEX region (Fig. 14A-B). We stress that this represents *potential* accumulation, as ice divergence, blowing snow and snow-ice formation will reduce the actual snow accumulation (Maksym and Markus, 2008). In addition, some

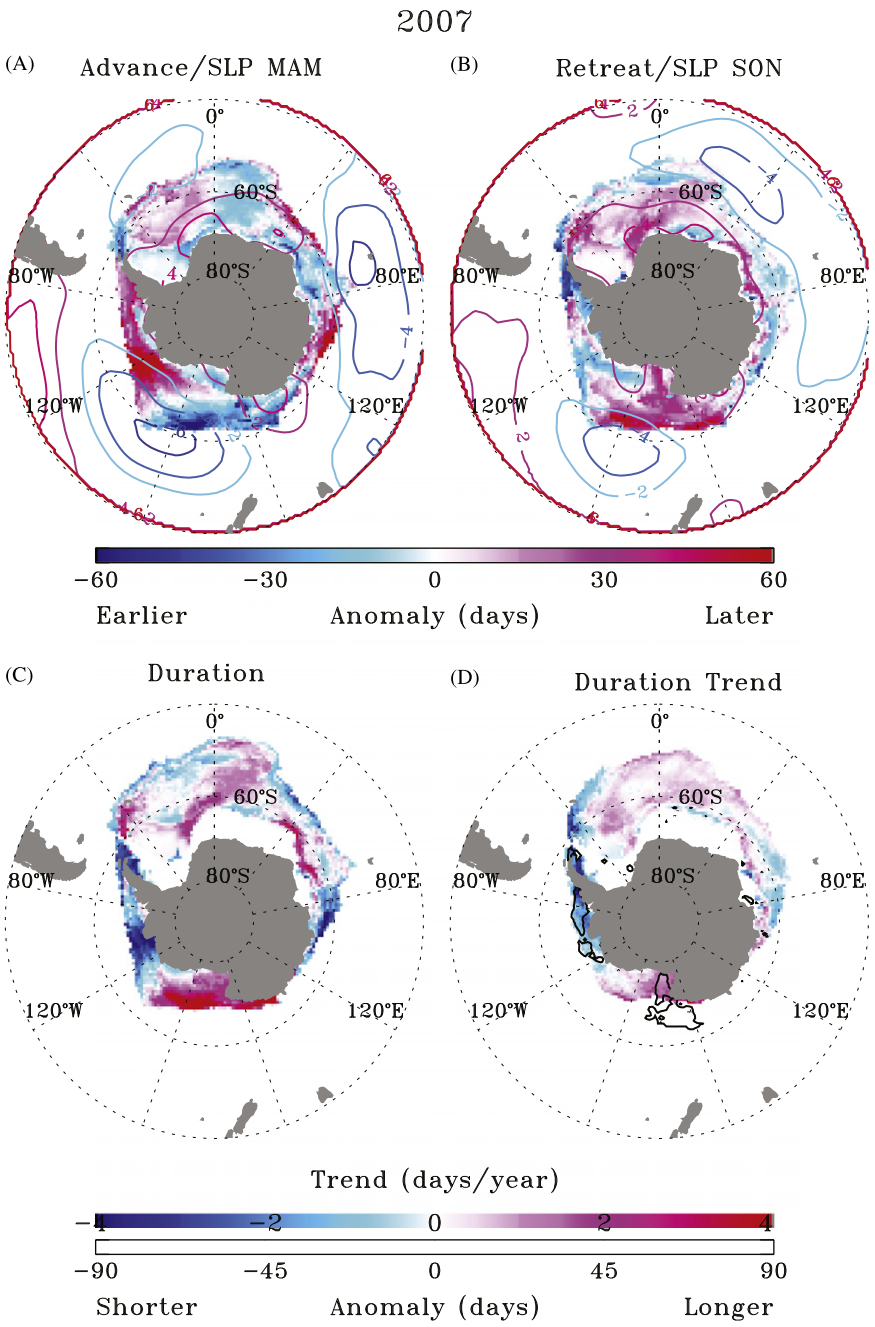

Fig. 11. Year 2007 circumpolar anomalies (based on 1979-80 to 2007-08) in the (A) timing of sea ice advance (B) timing of sea-ice retreat (C) ice season duration, and (D) the 1979-80 to 2007-08 trend in ice season duration (the black contour delimits the 0.01 significance level). Color contours in (A) and (B) correspond to seasonal sea-level pressure anomalies for March-April-May and September-October-November, respectively (i.e. the months during which sea ice begins its advance and retreat, respectively).

of this precipitation may have been liquid, which also may have a negative influence on snow depth (Massom et al., 2001).

Next, we present the evolution of the satellite-derived snow depth (Fig. 15). For the SIMBA region, deep snow in 2007 was initially restricted to the west of the study area and north of Thurston Island (72.1°S, 99.0°W). This feature, as observed in May (Fig. 15A), extended into the Amundsen Sea and was a band of multi-year sea ice. Of note is the apparent increase in size of this band and deepening snow in July (Fig. 15C). The sea-ice drift information does not suggest that the band moved significantly eastward. Rather, sea ice was advected northwards away from the coast in June and July (Fig. 6B and C). The increase in sea-ice concentration in the interior pack in July (Fig. 10C) suggests that there was widespread convergence, so precipitation would have increased the average snow depth (i.e., less lost into leads through openings in the ice cover). A subsequent decrease in snow depth in August (Fig. 15D) reflected the anomalously high export of sea ice from the Bellingshausen Sea to the Amundsen Sea (Fig. 6D). The net effect of ice export and reduced snowfall leading up to September contributed to negative September snow depth anomalies (up to ~0.08 m, Fig. 16A) in the Bellingshausen Sea. The SIMBA study region itself was located in the transition region between negative and positive snow depth anomalies to the east and west of 90°W (Fig. 16), where *in situ* measurements at SIMBA in October showed average to above average snow depths (Lewis et al., 2011).

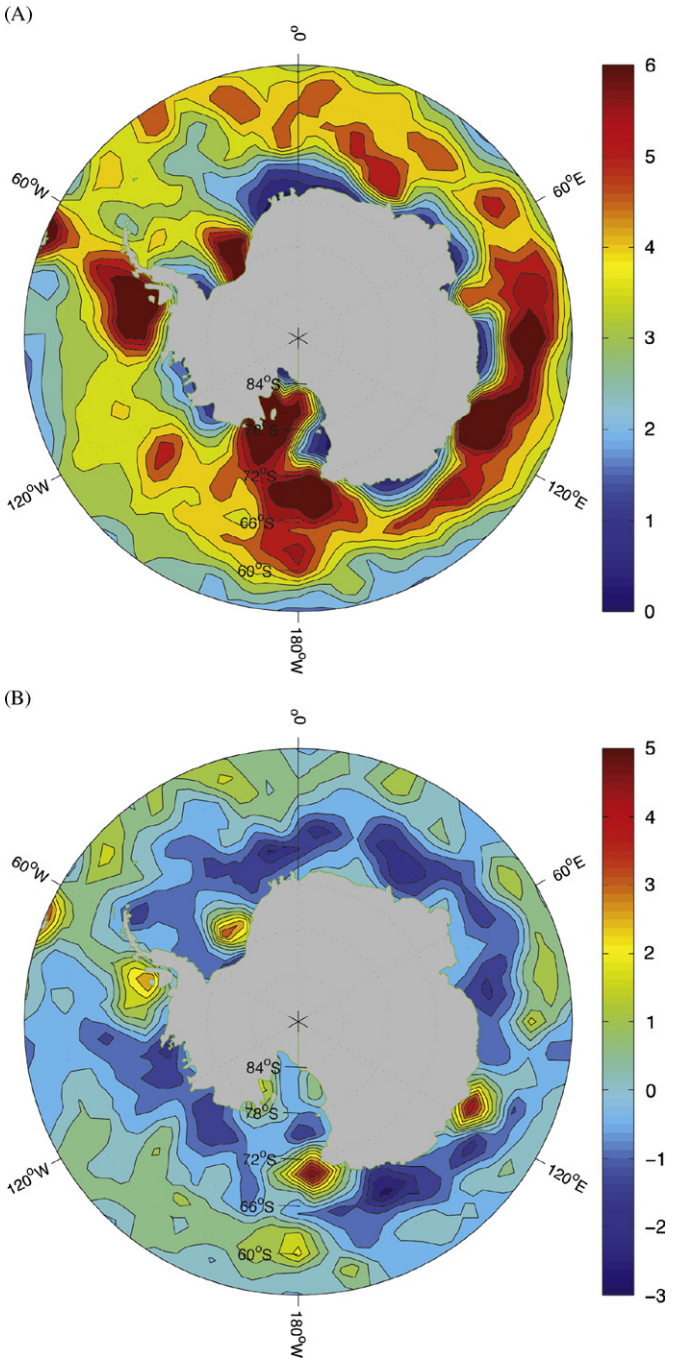

Fig. 12. Year 2007 circumpolar cyclone density (A) mean and (B) anomaly (based on 1979-2008). The anomalies in the SIMBA and SIPEX region deviate more than ± 2 standard deviations from the mean.

In the SIPEX region, snow depths were generally between 0.10-0.15 m and in September-October snow-depth anomalies were near zero or slightly negative (Fig. 16). Passive microwave snow depth is known to underestimate snow depth in the East Antarctic sector (Worby et al., 2008a). However, the 2007 SIPEX snow depths (Fig. 15) are comparable to previous observations of springtime snow depths (albeit limited) given by Massom et al. (2001) and Worby et al. (1998). Mean snow depth in 2007 did not change significantly between July and September despite the high precipitation rate. The contrast between high precipitation and relatively thin snow cover was previously noted for this region (Maksym and Markus, 2008) and is discussed further below.

4. Discussion

The most recent estimates of Antarctic monthly sea-ice extent changes over 1978-2006 (Cavalieri and Parkinson, 2008; Comiso and Nishio, 2008) show an overall increasing trend of $+0.9 \pm 0.2\%$ per decade, though regionally the two largest but opposing trends are in the Ross Sea (+4.2% per decade) and Bellingshausen and Amundsen seas (-5.7% per decade) (Comiso and Nishio, 2008). Further, circumpolar averaged sea-ice extent in September 2007 was the second highest (after 2006) based on our analysis of the 1979-2007 record. Somewhat coincidentally SIMBA and SIPEX happened to sample the two regions showing the largest negative sea-ice anomalies in the Southern Ocean in 2007. As illustrated above, the sea-ice conditions encountered during SIMBA and SIPEX resulted from a complex interplay between winds, surface ocean conditions, snowfall, sea-ice drift and deformation. Here, we discuss the implications of the regional ice-atmosphere-ocean anomalies on snow distribution in particular, and then we discuss the known climate conditions during IPY 2007.

4.1. Implications of Precipitation, Delayed Sea-Ice Advance and Sea-Ice Drift on Snow-Depth Anomalies

In general, estimates of precipitation from atmospheric reanalysis indicate particularly high amounts in the SIMBA and SIPEX study areas (e.g., Cullather et al., 1998), although the effects on snow and sea-ice mass balance differ somewhat between the two regions. Sea ice in the Bellingshausen Sea is characterized by relatively deep snow (Adolphs, 1998; Worby et al., 1996), and a large snow-ice fraction (Jeffries et al., 2001). East Antarctic sea ice typically has somewhat thinner snow and less snow-ice formation (Worby et al., 1998). Ship-based observations indicate that the greatest contrasts between the SIMBA and SIPEX regions occur in summer (Worby et al., 2008b), whereas those derived from satellite passive microwave observations indicate greater contrasts year-round (Markus and Cavalieri, 1998). The latter may partly reflect the effects of variable amounts (year-to-year) of multi-year sea ice in the Bellingshausen Sea on the snow-depth retrieval algorithm.

As shown here for year 2007, the relationship between precipitation and accumulation is modest and depends on the relative timing of precipitation events and sea-ice advance. Further, the regionally-averaged snow depth is also a function of the snow-to-ice conversion rate and the rate of new ice production, which initially has no snow cover and so reduces the mean snow depth (Maksym and Markus, 2008). Thus, differences in snow depth and snow-ice formation rates between the SIMBA and SIPEX regions may be partly due to higher rates of divergence and new ice formation in the East Antarctic pack ice compared to the southern Bellingshausen Sea.

For the SIMBA region, low precipitation leading up to September (Fig. 13), low initial sea-ice extent (Fig. 5), and increased sea-ice export (Fig. 6) all contributed to low snow depth during SIMBA (Figs. 15 and 16). How this might affect the ice mass balance is unclear. While thin snow could promote sea-ice growth due to the decreased insulation from cold winter air temperatures, it might also lead to decreased flooding and low rates of snow-ice production, thus contributing less to ice thickening. As mentioned, blowing snow may also have contributed to the thin snow cover that was observed on level ice at SIMBA (Leonard and Cullather, 2008).

Despite higher-than-average precipitation in the western SIPEX region in the months leading up to the experiment (Fig. 13), snow depth did not increase significantly (Figs. 15 and 16). This may indicate an increased rate of snow-ice formation. SIPEX observations show that about 8-18% of the pack ice was snow

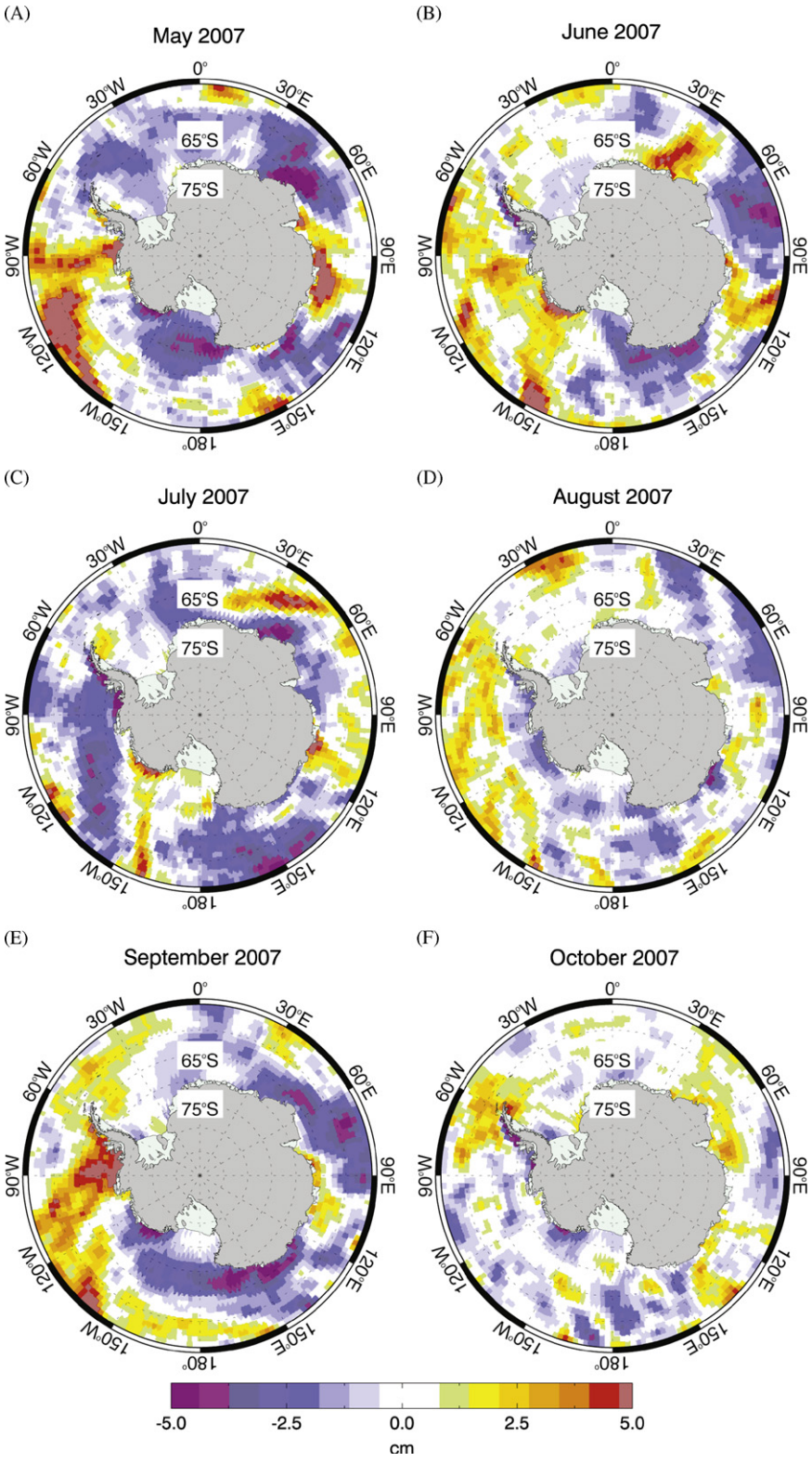

Fig. 13. May-October 2007 ECMWF precipitation anomalies (based on 1989-2007). Units are in cm water equivalent.

ice (Meiners et al., 2011; van der Merwe et al., 2009), which is at the lower end of the range derived from prior data collected in the East Antarctic pack ice (Massom et al., 2001). Hence, snow depth here may largely be independent of the accumulation rate and determined more by the rate of ice divergence (Heil et al., in press).

4.2. Climate Anomalies in 2007

The positive SST anomalies in the greater SIMBA and western SIPEX regions seen in May 2007 (Fig. 10A) were apparent as early as February (not shown) and similarly extended from mid-to-high latitudes. During February, the SST anomalies were coincident with

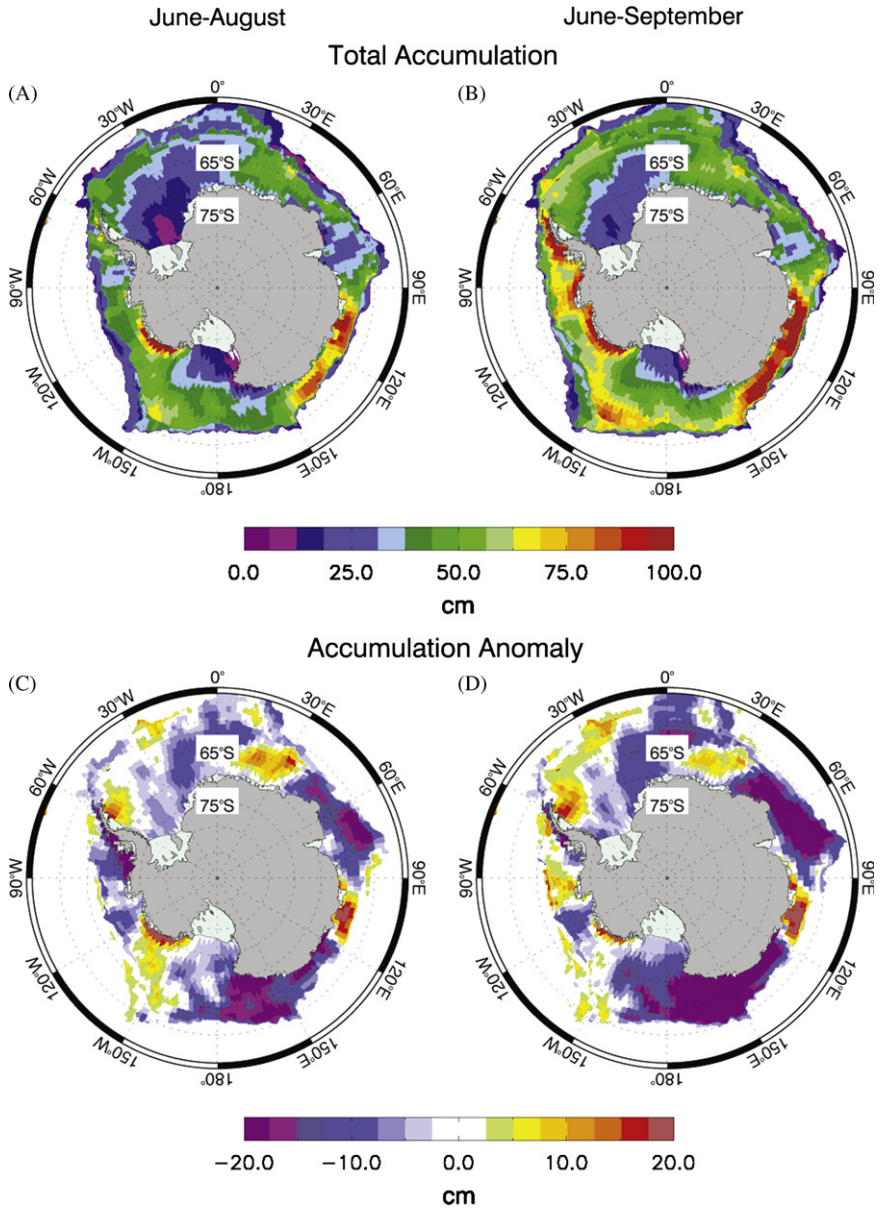

Fig. 14. Potential total snow accumulation as represented by total precipitation over sea-ice, integrated over: (A) June-August, (B) June-September and corresponding anomalies (C) June-August, (D) June-September. Units are in cm of snow equivalent using an assumed density of 350 kg m^{-3} (based on Massom et al., 2001) for direct comparison to snow depth (e.g., Fig. 13).

two high-pressure (blocking) anomalies centered southwest of New Zealand (55°S, 150°E) and west of southern South America (55°S, 100°W) that are apparent even in seasonal (January-April) averages (see Figure 5.22 a,b in Levinson and Lawrimore, 2008). These blocking highs led to the incursion of warm air into high latitudes along their western limbs and likely contributed to the observed positive SST anomalies. As the Southern Hemisphere transitioned into autumn, storm tracks intensified southward in accordance with the Semi-Annual Oscillation (van Loon, 1967), revealing a wave-3 pattern (Raphael, 2004) in SLP for the March-April-May seasonal mean (Fig. 11A). The deep low pressure anomalies centered on 160°W and 90°E continued delivering warm northerly winds to the SIMBA and SIPEX regions, contributing to the southward extension of warm SSTs observed in May (Fig. 10A). Together with converging (northerly) winds (Figs. 5 and 7) and inferred summer solar ocean warming (due to anomalously long ice-free summers in these regions, Fig. 9), autumn sea-ice advance was delayed (Fig. 11A). The wave-3 pattern weakened slightly during winter (June-July-August, not shown), then strengthened somewhat again during spring (September-October-November, Fig. 11B), thus assisting in the persistent negative ice-edge anomalies and warm-ocean conditions in these regions.

The year 2007 was therefore quite unusual in that the warm SST pattern in the greater SIMBA and SIPEX regions persisted for most of the year, regionally intensified by an atmospheric wave-3 pattern developed in austral autumn and was in turn facilitated by an overall weaker zonal (westerly) circulation (Marshall, 2007). Indeed, year 2007 marked a hiatus in the trend towards a more positive Southern Annular Mode (SAM) with its associated strengthened circumpolar westerly winds (Marshall, 2003). From March to October, the SAM was negative and the westerly circulation was relatively weak, until late in the year (December) (Levinson and Lawrimore, 2008), when the SAM became positive again. In short, the weakened zonal circulation allowed for stronger meridional circulation, first in association with the blocking highs in February and then in association with the wave-3 pattern in the

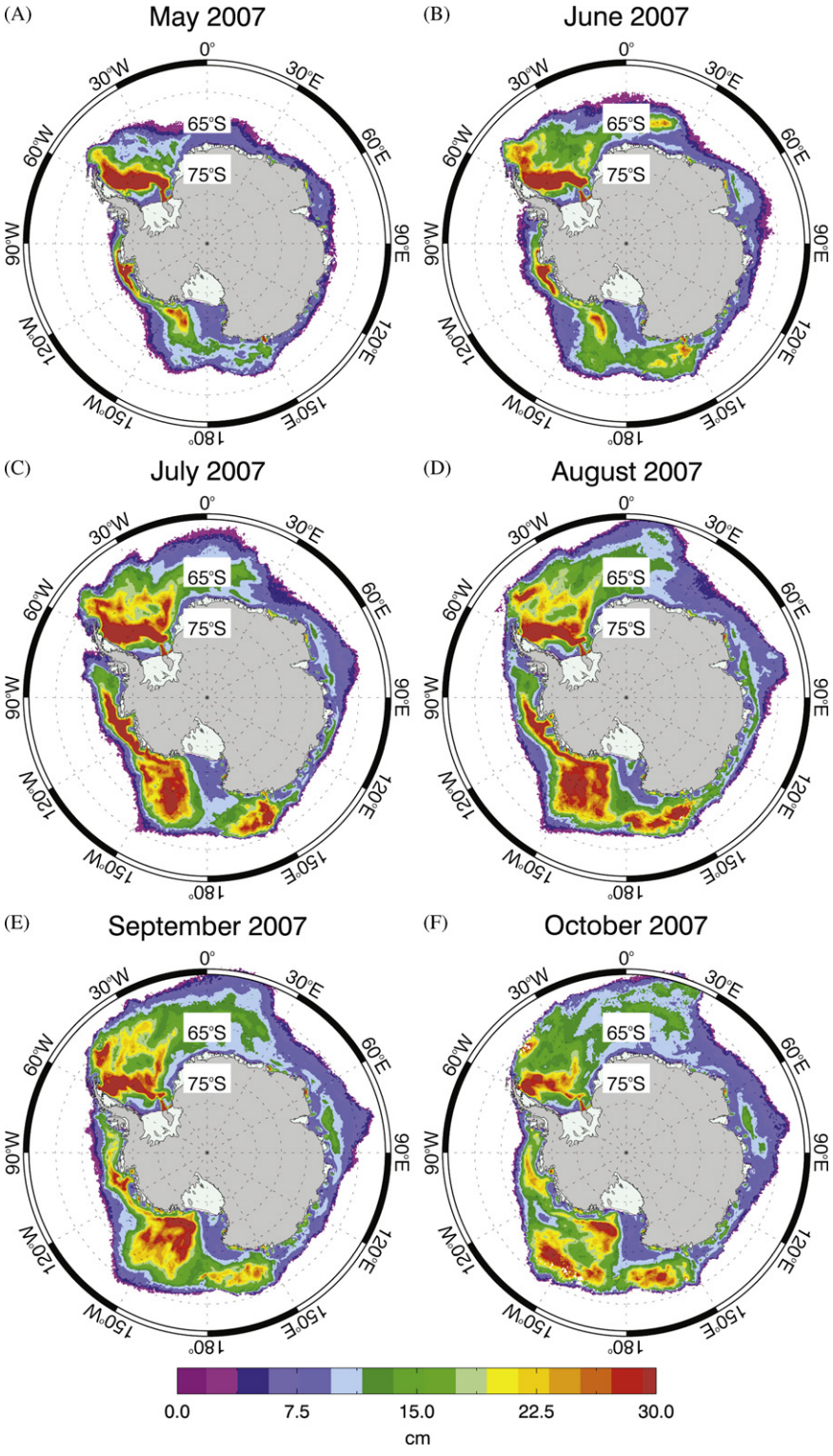

Fig. 15. May-October SSM/I-derived snow depth on sea ice.

subsequent autumn and spring. As a consequence, there was enhanced southward penetration of warm maritime air, reaching even the continental interior, where warming exceeded 2 standard deviations in the mid-to-lower troposphere (see Fig 5.21 in Levinson and Lawrimore, 2008).

The atmospheric circulation anomalies in 2007 helped to explain the anomalous sea-ice conditions in the western SIPEX region in particular, where annual se-ice extent in 2007 was a negative departure from an otherwise slightly positive trend. The positive trend in sea ice, almost everywhere but in the Bellingshausen and eastern Amundsen Seas, has been explained as resulting from a more positive SAM and stronger westerly winds, which contribute to positive ice-edge anomalies via wind-driven northward sea-ice drift (e.g., Stammerjohn et al., 2008). In contrast, in the Bellingshausen and eastern Amundsen sea regions, a more positive SAM is associated with intensified atmospheric low

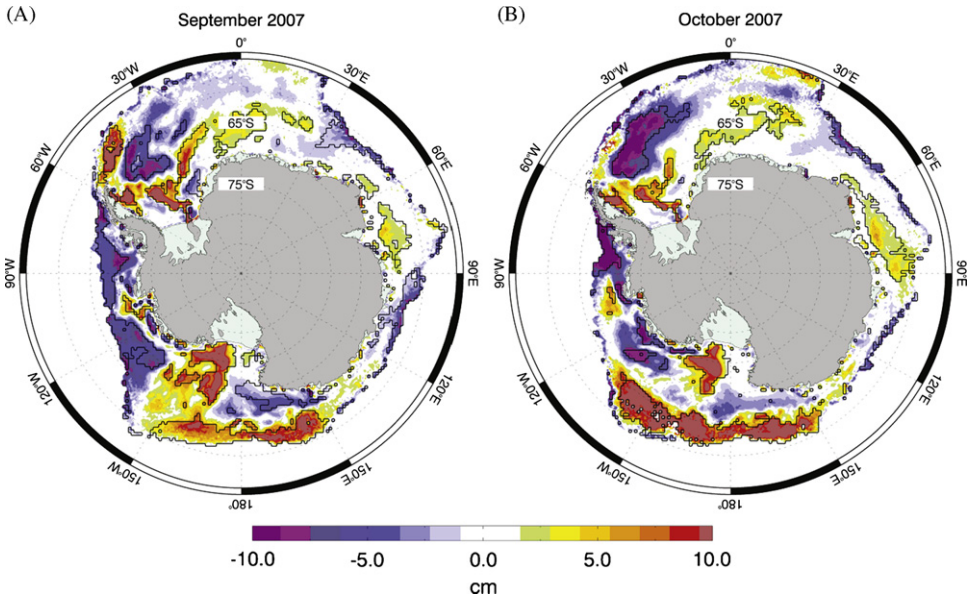

Fig. 16. Snow depth anomaly (based on 1989-2007) for (A) September, and (B) October. The black contours enclose those anomalies with greater than ± 1 standard deviation.

pressure anomalies in the high-latitude southeast Pacific Ocean (Fogt and Bromwich, 2006; Lefebvre et al., 2004), i.e. intensifying the Amundsen Sea Low (Turner et al., 2009). This increases northerly winds west of the Antarctic Peninsula and decreases sea-ice coverage in the Bellingshausen and eastern Amundsen seas (Massom et al., 2006; Massom et al., 2008). Interestingly, and in spite of the negative SAM, year 2007 also showed increased northerly winds into this region, but these resulted from the wave-3 pattern. Therefore, year 2007 saw a continuation of the downward trend in sea ice in this region. Similar conditions occurred in the Bellingshausen Sea in spring 2005 (Massom et al., 2008).

5. Summary

Here, we presented an assessment of the ice-atmosphere-ocean conditions leading up to and during two springtime field campaigns, SIMBA and SIPEX, so that we could better understand sea-ice conditions encountered during IPY 2007 and evaluate their representativeness. We focused on the general correspondence between winds, sea-ice extent and drift, and how these interactions related to atmospheric circulation anomalies, surface ocean conditions and the delivery of precipitation, to arrive at some understanding of the regional differences in snow and sea-ice distributions. A strong factor in shaping the sea-ice conditions observed during the field campaigns in September and October was the wind-driven delays (by up to 2 months) in sea-ice advance in the SIMBA and western SIPEX regions, while the eastern SIPEX region experienced near to above normal sea-ice advance (Fig. 11). Maps of sea-surface temperature (SST) and sea ice concentration (SIC) anomalies (Fig. 10) revealed distinct regional patterns, showing warm SST/low SIC in the greater SIMBA (including all of the Bellingshausen and Amundsen seas) and western SIPEX regions, versus cool SST/high SIC in the Weddell, Ross and eastern SIPEX regions. In the SIMBA and western SIPEX regions warm northerly winds in May (Figs. 5 and 7A) overlying the warm SSTs brought anomalously high precipitation to these regions (Fig. 13), but most fell on open ocean due to the regional delays in sea-ice advance.

When sea-ice advance did occur in the greater SIMBA region, it was assisted by southerly winds (Fig. 5) and northward sea-ice drift (Fig. 6). Yet, the ice edge remained south of its mean (1979-2007) position (Fig. 5), suggesting an influence by the anomalously warm ocean conditions (Fig. 10) intensified perhaps by increased solar ocean warming during the long preceding ice-free summer period (Fig. 9). In contrast, in the western SIPEX region, the late sea-ice advance was assisted by easterly winds (Fig. 7) and westward sea ice drift (Fig. 8), which brought positive sea-ice anomalies from the east. Nonetheless, the ice edge just west of SIPEX also remained south of its mean (1979-2007) position (Fig. 7), again suggesting an influence by the anomalously warm ocean conditions observed there (Fig. 10). In addition, the preceding summer open-water period in the SIPEX region was the 2nd longest observed over 1979-2007, inferring a large relative increase in solar ocean warming.

Following sea-ice advance, in the SIMBA region there was a strong positive precipitation anomaly in September, while in the western SIPEX region precipitation anomalies were positive to slightly positive from June through September. Nonetheless, snow-depth anomalies on sea ice in September and October were strongly negative in the greater SIMBA region and negative to zero in the SIPEX region. This resulted from a combination of factors, particularly the delayed timing of sea-ice advance, but was also likely caused by the redistribution of snow by winds (concentrating it into relatively small areas or into openings within the pack ice) and by sea-ice drift and deformation processes, and as well as the loss of snow to snow-ice formation.

In short, the relatively thin snow and preponderance of young sea ice in the SIMBA region in 2007 stood in stark contrast to the deep snow and heavy multi-year sea ice that plagued this region's early explorers in the late 1800s. It also contrasts with relatively deep snow encountered in this region more recently (e.g., Massom et al., 2006; Perovich et al., 2004; Worby et al., 1996). The satellite-derived sea-ice record shows, however, that since the late 1980s, there is frequently less to no summer sea ice in the southeastern Bellingshausen Sea, while sea-ice extent, duration, and concentration have decreased dramatically (Comiso and Nishio, 2008; Jacobs and Comiso, 1997; Stammerjohn et al., 2008). One consequence of these changes is overall less multiyear sea ice in the Bellingshausen Sea, and in 2007 the relatively small band of multi-year sea ice that was present in the western Bellingshausen Sea was exported to the Amundsen Sea (Fig. 1A, Maksym, unpublished data).

In the SIPEX region, year 2007 was differently distinguished by being a significant negative departure from an otherwise slightly

positive increasing trend in this region. The east-west contrasts in sea-ice extent, concentration and drift was particularly striking and reflected the anomalous meridional influence of a wave-3 atmospheric circulation pattern against a relatively weakened westerly circulation. Also noteworthy was the anomalously long ice-free summer period and warm SSTs prior to SIPEX, with inferred impacts on the coastal network of fast ice (Giles et al., 2008) during the 2006-07 summer and negative ice-edge anomalies in the western SIPEX region during the subsequent autumn and winter in 2007.

Acknowledgments

Participation on SIMBA by SS and KL was under the auspices of NSF/OPP grants ANT-07-03682 (PI S.F. Ackley, UTAS) and ANT-06-32282 (P.I. S.S. Jacobs, LDEO), during which SS was a NOAA Climate and Global Change Postdoctoral Fellow, administered by the University Corporation for Atmospheric Research. For PH and RM, this work contributes to the Australian Antarctic Science projects 742, 2678, 2901 and 3204, and was supported by the Australian Government's Cooperative Research Centres Programme through the Antarctic Climate and Ecosystems Cooperative Research Centre. MV was supported by FRFC-FNRS (Sea-ice biogeochemistry in polar oceans). TM thanks the British Antarctic Survey, and Gareth Marshall and Tony Phillips for processing the precipitation data and assistance with the production of figures. The GSFC SMMR-SSM/I sea-ice concentration data were from the EOS Distributed Active Archive Center (DAAC) at the National Snow and Ice Data Center, University of Colorado in Boulder, Colorado (http://nsidc.org). The sea-level pressure and 10-m wind data were from the National Center for Environmental Prediction/National Center for Atmospheric Research Reanalysis Project (http://www.cdc.noaa.gov). Precipitation was derived from the European Centre for Medium range Weather Forecasts (ECMWF) interim reanalysis (www.ecmwf.int/research/era/do/get/era-interim). The International Research Institute for Climate Prediction (http://iridl.ldeo.columbia.edu/) provided the sea-surface temperature data produced by Reynolds et al. (2002). Chuck Fowler (Colorado Center for Astrodynamics Research, University of Colorado) is thanked for providing the satellite-derived sea-ice motion product. We thank Stan Jacobs, Steve Ackley, Tony Worby, Cathy Geiger and Rich Cullather for discussions relating to this paper. Finally we thank the ships' captain, crew, and logistical support during the U.S.- and Australian-led IPY field studies.

References

Adolphs, U., 1998. Ice thickness variability, isostatic balance and potential for snow ice formation on ice floes in the south polar Pacific Ocean. Journal of Geophysical Research 103 (C11), 24675–24691.

Assmann, K.M., Hellmer, H.H., Jacobs, S.S., 2005. Amundsen Sea ice production and transport. Journal of Geophysical Research, 110. doi:10.1029/2004JC002797.

Bromwich, D.H., Fogt, R.L., Hodges, K.I., Walsh, J.E., 2007. A tropospheric assessment of the ERA-40, NCEP and JRA-25 global reanalyses in the polar regions. Journal Geophysical Research 112 (D10111. doi:10.1029/2006JD007859.

Cavalieri, D.J., Parkinson, C.L., 2008. Antarctic sea ice variability and trends, 1979–2006. Journal Geophysical Research 113 (C07004. doi:10.1029/2007JC004564.

Comiso, J.C., 1999. Bootstrap sea ice concentrations from NIMBUS-7 SMMR and DMSP SSM/I 1979-2007. Boulder, Colorado USA: National Snow and Ice Data Center. Digital media.

Comiso, J.C., Nishio, F., 2008. Trends in the sea ice cover using enhanced and compatible AMSR-E, SSM/I, and SMMR data. Journal of Geophysical Research, 113. doi:10.1029/2007JC004257.

Cullather, R.I., Bromwich, D.H., Van Woert, M.L., 1998. Spatial and temporal variability of Antarctic precipitation from atmospheric methods. Journal of Climate 11, 334–367.

Fichefet, T., Morales Maqueda, M.A., 1999. Modelling the influence of snow accumulation and snow-ice formation on the seasonal cycle of the Antarctic sea-ice cover. Climate Dynamics 15, 251–268.

Fichefet, T., Tartinville, B., Goosse, H., 2000. Sensitivity of the Antarctic sea ice to the thermal conductivity of snow. Geophysical Research Letters 27, 401–404 doi:410.1029/1999GL002397.

Fogt, R.L., Bromwich, D.H., 2006. Decadal variability of the ENSO teleconnection to the high latitude South Pacific governed by coupling with the Southern Annular Mode. Journal of Climate 19, 979–997.

Fowler, C., 2003. Polar Pathfinder Daily 25 km EASE-Grid Sea Ice Motion Vectors. updated 2007. National Snow and Ice Data Center, Boulder, Colorado USA.

Fritsen, C.H., Lytle, V.I., Ackley, S.F., Sullivan, C.W., 1994. Autumn bloom of Antarctic pack-ice algae. Science 266 (5186), 782–784 doi:710.1126/science.1266.5186.1782.

Giles, A.B., Massom, R.A., Lytle, V.I., 2008. Fast ice distribution in East Antarctica during 1997 and 1999 determined using Radarsat data. Journal of Geophysical Research 113 (C02S14. doi:10.1029/2007JC004139.

Gloersen, P., Campbell, W.J., Cavalieri, D.J., Comiso, J.C., Parkinson, C.L., Zwally, H.J., 1992. Arctic and Antarctic Sea Ice, 1978-1987: Satellite Passive-Microwave Observations and Analysis. National Aeronautics and Space Administration, Washington, DC.

Harangozo, S.A., 2004. The impact of winter ice retreat on Antarctic winter sea-ice extent and links to the atmospheric meridional circulation. International Journal of Climatology 24, 1023–1044.

Harangozo, S.A., 2006. Atmospheric circulation impacts on winter maximum sea ice extent in the west Antarctic Peninsula region (1979-2001). Geophysical Research Letters, 33. doi:10.1029/2005GL024978.

Heil, P., Allison, I., 1999. The pattern and variability of Antarctic sea-ice drift in the Indian Ocean and western Pacific sectors. Journal of Geophysical Research 104 (C7), 15789–15802.

Heil, P., Allison, I., Massom, R.A., Worby, A.P., Effects of intensified atmospheric forcing and near-coastal currents on meso-scale sea-ice dynamics off East Antarctica. Deep-Sea Research II, in press.

Jacobs, S.S., Comiso, J.C., 1993. A recent sea-ice-retreat west of the Antarctic Peninsula. Geophysical Research Letters 20 (12), 1171–1174.

Jacobs, S.S., Comiso, J.C., 1997. Climate variability in the Amundsen and Bellingshausen Seas. Journal of Climate 10, 697–709.

Jeffries, M.O., Krouse, H.R., Hurst-Cushing, B., Maksym, T., 2001. Snow-ice accretion and snow-cover depletion on Antarctic first-year sea-ice floes. Annals of Glaciology 33, 51–60.

Kalnay, E., Kanamitsu, M., Kistler, R., Collins, W., Deaven, D., Gandin, L., Iredell, M., Saha, S., White, G., Woollen, J., Zhu, Y., Chelliah, M., Ebisuzaki, W., Higgins, W., Janowiak, J., Mo, K.C., Ropelewski, C., Wang, J., Leetmaa, A., Reynolds, R., Jenne, R., Joseph, D., 1996. The NCEP/NCAR 40-year reanalysis project. Bulletin of American Meteorological Society 77, 437–471.

Lefebvre, W., Goosse, H., Timmermann, R., Fichefet, T., 2004. Influence of the Southern Annular Mode on the sea ice-ocean system. Journal of Geophysical Research, 109. doi:10.1029/2004JC002403.

Leonard, K.C., Cullather, R.I., 2008. Snowfall measurements in the Amundsen and Bellingshausen Seas, Antarctica. Proceedings of the 6th Eastern Snow Conference, Fairlee, VT, USA, pp. 87–98.

Levinson, D.H., Lawrimore, J.H. (Eds.), 2008. Bulletin of the American Meteorological Society, Special supplement, 89; 2008, pp. S97–S106.

Lewis, M., Tison, J., Weissling, B., Delille, B., Ackley, S., Brabant, F., Xie, H., 2011. Sea ice and snow cover characteristics during the winter spring transition in the Bellingshausen Sea: an overview of SIMBA 2007. Deep-Sea Research II 58 (9–10), 1019–1038.

Maksym, T., Jeffries, M.O., 2000. A one-dimensional percolation model of flooding and snow ice formation on Antarctic sea ice. Journal Geophysical Research 105 (26), 313–326 doi:310.1029/2000JC900130.

Maksym, T., Markus, T., 2008. Antarctic sea ice thickness and snow-to-ice conversion from atmospheric reanalysis and passive microwave snow depth. Journal Geophysical Research 113 (C02S12. doi:10.1029/2006JC004085.

Markus, T., Cavalieri, D.J., 1998. Snow depth distribution over sea ice in the Southern Ocean from passive microwave data. In: Jeffries, M.O. (Ed.), Antarctic Sea Ice: Physical Processes, Interactions and Variability. AGU, Washington, D.C, pp. 19–39.

Markus, T., Cavalieri, D.J., 2006. Interannual and regional variability of Southern Ocean snow on sea ice. Journal of Glaciology 44 (1), 53–57. doi:10.3189/172756406781811475.

Markus, T., Powell, D.C., Wang, J.R., 2006. Sensitivity of passive microwave snow depth retrievals to weather effects and snow evolution. Transactions of Geosciences and Remote Sensing 44, 66–77. doi:10.1109/TGRS.2005.860208.

Marshall, G.J., 2003. Trends in the Southern Annular Mode from observations and reanalyses. Journal of Climate 16, 4134–4143.

Marshall, G.J., 2007. Half-century seasonal relationships between the southern annular mode and Antarctic temperatures. International Journal of Climatology 27, 373–383.

Marshall, G.J., 2009. On the annual and semi-annual cycles of precipitation across Antarctica. International Journal of Climatology 29, 2298–2308 doi:2210.1002/joc.1810.

Maslanik, J., Stroeve, J., 1999. Near-Real-Time DMSP SSM/I Daily Polar Gridded Sea Ice Concentrations. 2008. Boulder, Colorado USA: National Snow and Ice Data Center. Digital media.

Massom, R.A., Harris, P.T., Michael, K., Potter, M.J., 1998. The distribution and formative processes of latent heat polynyas in East Antarctica. Annals of Glaciology 27, 420–426.

Massom, R.A., Comiso, J.C., Worby, A.P., Lytle, V.I., Stock, L., 1999. Satellite and in situ observations of regional classes of sea ice cover in the East Antarctic pack in winter. Remote Sensing of the Environment 68 (1), 61–76.

Massom, R.A., Eicken, H., Haas, C., Jeffries, M.O., Drinkwater, M.R., Sturm, M., Worby, A.P., Wu, X., Lytle, V.I., Ushio, S., Morris, K., Reid, P.A., Warren, S.G., Allison, I., 2001. Snow on Antarctic Sea Ice. Reviews of Geophysics 39 (3), 413–445.

Massom, R.A., Stammerjohn, S.E., Smith, R.C., Pook, M.J., Iannuzzi, R., Adams, N., Martinson, D., Vernet, M., Fraser, W.R., Quetin, L.B., Ross, R.M., Massom, Y., Krouse, H.R., 2006. Extreme anomalous atmospheric circulation in the west Antarctic Peninsula region in austral spring and summer 2001/2, and its profound impact on sea ice and biota. Journal of Climate 19, 3544–3571.

Massom, R.A., Stammerjohn, S.E., Lefebvre, W., Harangozo, S.A., Adams, N., Scambos, T., Pook, M.J., Fowler, C., 2008. West Antarctic Peninsula sea ice in 2005: extreme compaction and ice edge retreat due to strong anomaly with respect to climate. Journal of Geophysical Research, 113. doi:10.1029/2007JC004239.

Meiners, K.M., Norman, L., Granskog, M.A., Krell, A., Heil, P., Thomas, D.N., 2011. Physico-ecobiogeochemistry of East Antarctic pack ice during the winter-spring transition. Deep-Sea Research II 58 (9–10), 1172–1181.

Murray, R.J., Simmonds, I., 1991. A numerical scheme for tracking cyclone centres from digital data. Part I: Development and operation of the scheme. Australian Meteorological Magazine 39, 155–166.

Perovich, D.K., Elder, B.C., Claffey, K.J., Stammerjohn, S., Smith, R., Ackley, S.F., Krouse, H.R., Gow, A.J., 2004. Winter sea ice properties in Marguerite Bay, Antarctica. Deep Research II 51, 2023–2039.

Raphael, M.N., 2004. A zonal wave 3 index for the Southern Hemisphere. Geophysical Research Letters 31 (L23212. doi:10.1029/2004GL020365.

Reynolds, R.W., Rayner, N.A., Smith, T.M., Stokes, D.C., Wang, W., 2002. An Improved In Situ and Satellite SST Analysis for Climate. Journal of Climate 15, 1609–1625.

Simmonds, I., 2003. Modes of atmospheric variability over the Southern Ocean. Journal of Geophysical Research, 108. doi:10.1029/2000JC000542.

Stammerjohn, S.E., Martinson, D.G., Smith, R.C., Yuan, X., Rind, D., 2008. Trends in Antarctic annual sea ice retreat and advance and their relation to ENSO and Southern Annular Mode Variability. Journal of Geophysical Research, 113. doi:10.1029/2007JC004269.

Sturm, M., Morris, K., Massom, R., 1998. The winter snow cover of the west Antarctic pack ice: Its spatial and temporal variability. In: Jeffries, M.O. (Ed.), Antarctic Sea Ice: Physical Processes, Interactions and Variability. AGU, Washington, D.C, pp. 1–18.

Sturm, M., Massom, R.A., 2009. Snow and sea ice. In: Thomas, D., Dieckmann, G. (Eds.), Sea Ice 2nd Edition Wiley-Blackwell, Oxford, pp. 153–204.

Toyota, T., Massom, R., Tateyama, K., Tamura, T., Fraser, A., 2011. Snow on Antarctic sea ice - results from SIPEX and SIMBA. Deep-Sea Research II, in press.

Turner, J., Comiso, J.C., Marshall, G., Lachlan-Cope, T.A., Bracegirdle, T., Maksym, T., Meredith, M.P., Wang, Z., Orr, A., 2009. Non-annular atmospheric circulation change induced by stratospheric ozone depletion and its role in the recent increase of Antarctic sea ice extent. Geophysical Research Letters 36, L08502. doi:10.1029/2009GL037524.

van der Merwe, P., Lannuzel, D., Mancuso Nichols, C.A., Meiners, K., Heil, P., Norman, L., Thomas, D.N., Bowie, A.R., 2009. Biogeochemical observations during the winter-spring transition in East Antarctic sea ice: Evidence of iron and exopolysaccharide controls. Mar. Chem. doi:10.1016/j.marchem.2009.1008.1001.

van Loon, H., 1967. The half-yearly oscillations in middle and high southern latitudes and the coreless winter. Journal of the Atmospheric Sciences 24 (5), 472–486.

Vancoppenolle, M., Timmermann, R., Ackley, S.F., Fichefeta, T., Goosse, H., Heil, P., Lieser, J., Leonard, K.C., Nicolaus, M., Papakyriakou, T., Tison, J.-L., 2011. Assessment of radiation forcing data sets for large-scale sea ice models in the Southern Ocean. Deep-Sea Research II 58 (9–10), 1237–1249.

Worby, A.P., Jeffries, M.O., Weeks, W.F., Morris, K., Jaña, R., 1996. The thickness distribution of sea ice and snow cover during late winter in the Bellingshausen and Amundsen Seas, Antarctica. Journal of Geophysical Research 101 (C12), 28441–28455.

Worby, A.P., Massom, R.A., Allison, I., Lytle, V., Heil, P., 1998. East Antarctic sea ice: a review of its structure, properties and drift. In: Jeffries, M. (Ed.), Antarctic Sea Ice: Physical Processes, Interactions and Variability. American Geophysical Union, Washington, D.C, pp. 41–67.

Worby, A.P., Geiger, C.A., Paget, M.J., Van Woert, M.L., Ackley, S.F., DeLiberty, T.L., 2008a. Thickness distribution of Antarctic sea ice. Journal Geophysical Research 113 (C05S92. doi:10.1029/2007JC004254.

Worby, A.P., Markus, T., Steer, A.D., Lytle, V.I., Massom, R.A., 2008b. Evaluation of AMSR-E snow depth product over East Antarctic sea ice using in situ measurements and aerial photography. Journal Geophysical Research 113 (C05S94. doi:10.1029/2007JC004181.

Worby, A.P., Steer, A., Lieser, J., Galin, N., Yi, D., Allison, I., Heil, P., Massom, R.A., Zwally, H.J. Regional-scale sea ice and snow thickness distributions from in situ and satellite measurements over East Antarctic pack ice during the Sea Ice Physics and Ecosystem eXperiment (SIPEX). Deep-Sea Research II, in press.

Xie, H., Ackley, S.F., Yi, D., Zwally, H.J., Wagner, P., Weissling, B., Lewis, M., Ye, K., 2011. Sea ice thickness distribution of the Bellingshausen Sea from surface measurements and ICESat altimetry. Deep-Sea Research II 58 (9–10), 1039–1051.

Zwally, H.J., Comiso, J.C., Parkinson, C.L., Campbell, W.J., Carsey, F.D., Gloersen, P., 1983. Antarctic Sea Ice, 1973-1976: Satellite Passive-Microwave Observations. National Aeronautics and Space Administration, Washington, D.C.